

UNCLASSIFIED

AD NUMBER

AD904474

LIMITATION CHANGES

TO:

Approved for public release; distribution is unlimited.

FROM:

Distribution authorized to U.S. Gov't. agencies only; Test and Evaluation; AUG 1971. Other requests shall be referred to Naval Ship Research and Development Center, Bethesda, Maryland 20034.

AUTHORITY

USNSRDC per ltr, 24 Apr 1974

THIS PAGE IS UNCLASSIFIED



L  
AD 904474

(2)

CB

8-1473

ANALYSIS OF THE HOVER PERFORMANCE OF A  
HIGH-SPEED CIRCULATION CONTROL ROTOR

by

Robert M. Williams

COPY

AD No. DDG FIL

Distribution limited to U. S. Government agencies  
only; Test and Evaluation; August 1971. Other  
requests for this document must be referred to

[REDACTED]

AVIATION AND SURFACE EFFECTS DEPARTMENT  
NAVAL SHIP RESEARCH + DEVELOPMENT  
CENTER, BETHESDA, MD. 20034

Technical Note AL-221

August 1971

NAVAL  
SHIP  
RESEARCH  
AND  
DEVELOPMENT  
CENTER

BETHESDA  
MARYLAND  
20034

DDC  
RECEIVED  
OCT 30 1972  
D

ACCESSION for

RTIS	White Section	<input type="checkbox"/>
DOC	Buff Section	<input checked="" type="checkbox"/>
UNANNOUNCED		<input type="checkbox"/>

JUSTIFICATION .....

BY .....

DISPOSITION ..... 12

13

ANALYSIS OF THE HOVER PERFORMANCE  
OF A HIGH SPEED CIRCULATION CONTROL ROTOR

by

Robert M. Williams

This work was performed under sponsorship of the  
Office of Naval Research, Aeronautics, Code 461,  
under Project Order #1-0140, NR 212-204.

Distribution limited to U. S. Government agencies  
only; Test and Evaluation; August 1971. Other  
requests for this document must be referred to

*Naval Ship Research + Development  
Center, Bethesda, Md. 20034*

August 1971

Technical Note AL-221

## SUMMARY

A method for calculating in detail the hover performance of a circulation control rotor is described. Hover results for a typical high speed helicopter configuration are presented. The method includes such detailed effects as non-uniform inflow, internal ducting losses and experimental airfoil data modified for compressibility effects. The calculations were performed on an untwisted, constant chord blade with varying section properties. It is demonstrated that hover Figures of Merit on the order of 0.80 are obtainable with this rotor system at thrust coefficients of 0.020. An optimum collective pitch angle is determined for each thrust coefficient. A favorable effect of compressibility on Figure of Merit up to a tip Mach number of 0.7 is shown. The rotor achieves near uniform inflow at its optimum collective pitch angle. It is demonstrated that very good hover efficiency may be obtained with a circulation control rotor without incurring the usual solidity and twist design compromises for forward flight.

## TABLE OF CONTENTS

	Page
INTRODUCTION. . . . .	1
HOVER METHODOLOGY . . . . .	2
TOTAL POWER COMPUTATION . . . . .	2
INDUCED POWER . . . . .	3
CORIOLIS POWER (PUMPING POWER). . . . .	4
COMPRESSOR POWER AND DUCT LOSSES. . . . .	5
PROFILE POWER . . . . .	8
ROTOR GEOMETRY AND OPERATING CONDITIONS . . . . .	10
RESULTS . . . . .	12
EFFECT OF COLLECTIVE PITCH. . . . .	12
EFFECT OF SLOT HEIGHT . . . . .	12
EFFECT OF TIP MACH NUMBER . . . . .	13
EFFECT OF TIP MACH NUMBER AND DISC LOADING ON POWER LOADING. . . . .	13
CONCLUSIONS . . . . .	14
ACKNOWLEDGEMENT . . . . .	16
APPENDIX A - SECTION DATA . . . . .	17
REFERENCES. . . . .	18

## LIST OF FIGURES

Figure 1 - Hover Methodology . . . . .	21
Figure 2 - Comparison of Experiment with Lock-Goldstein Inflow Theory. . . . .	22
Figure 3 - Typical Radial Variation of Internal Flow Parameters in an Elliptical Cross Section Duct. . . . .	23
Figure 4 - Rotor Geometry. . . . .	24
Figure 5 - Variation of Hover Figure of Merit with Collec- tive Pitch and Thrust Coefficient . . . . .	25
Figure 6 - Variation of Power Components with Collective Pitch, $C_T = 0.010$ . . . . .	26
Figure 7 - Variation of Radial Load Distribution with Collective Pitch, $C_T = 0.010$ . . . . .	27
Figure 8 - Calculated Induced Velocity Distribution Corre- sponding to Lift Distributions of Figure 7 . . . . .	28

## LIST OF FIGURES (cont'd)

Figure 9 - Variation of Average Duct Flow Properties with Collective Pitch (For Rotor Parameters of Figures 5-8) . . . . .	29
Figure 10 - Effect of Slot Height on Locus of Optimum Hover Figure of Merit . . . . .	30
Figure 11 - Effect of Tip Mach Number on Figure of Merit. . . . .	31
Figure 12 - Variation of Figure of Merit with Collective Pitch (a) $M_{TIP} = 0.51$ . . . . .	32
(b) $M_{TIP} = 0.70$ . . . . .	33
(c) $M_{TIP} = 0.90$ . . . . .	34
Figure 13 - Variation of Power Loading with Disc Loading and Tip Mach Number . . . . .	35
Figure 14 - Comparison of Circulation Control Rotor and High Performance Conventional Rotors of Same Solidity ( $\sigma = 0.0819$ ) . . . . .	36
Figure A1 - Root Section Lift Characteristics . . . . .	37
Figure A2 - Tip Section Lift Characteristics. . . . .	38
Figure A3 - Root Section Drag Characteristics . . . . .	39
Figure A4 - Tip Section Drag Characteristics. . . . .	40
Figure A5 - Lift Compressibility Factor (a) $w/R_{TE} = 0.01209$ . . . . .	41
(b) $w/R_{TE} = 0.0323$ . . . . .	42
Figure A6 - Drag Compressibility (a) $w/R_{TE} = 0.01209$ . . . . .	43
(b) $w/R_{TE} = 0.0323$ . . . . .	44

# SYMBOLS

A	Area, $\text{ft}^2$
C	Chord, ft
$C_d$	Section drag coefficient
$C_l$	Section lift coefficient
$C_P$	Power coefficient
$C_P$	Specific heat at constant pressure, $\text{Btu}/\text{lb}_m - \text{deg F}$
$C_T$	Thrust coefficient, $T/\rho V_T^2 S$
$C_V$	Specific heat at constant volume, $\text{Btu}/\text{lb}_m - \text{deg F}$
$C_\mu$	Momentum coefficient, $\frac{\dot{m} V_j}{q A}$
$D_o$	Hydraulic diameter, ft
$\bar{f}$	Friction coefficient
F	Lift compressibility correlation factor
FM	Figure of Merit
g	Acceleration due to gravity, $32.17 \text{ ft}/\text{sec}^2$
$\dot{m}$	Mass flow rate, slugs/sec
M	Mach number
N	Number of blades
P	Power, $\text{ft-lb}/\text{sec}$
$P_e$	Compressor exit pressure, $\text{lb}/\text{ft}^2$
$P_o, P_d$	Pressure, $\text{lb}/\text{ft}^2$
q	Dynamic pressure, $\frac{1}{2} \rho V^2$
r	Local radius, ft
$\bar{r}$	Heat recovery factor

$R$	Radius, ft
$\bar{R}$	Gas constant, ft/ $^{\circ}$ R
$s$	Dummy integration variable
$S$	Rotor disc area, ft <sup>2</sup>
$T$	Temperature, deg R
$t/C$	Section thickness - chord ratio
$T/S$	Disc loading, lb/ft <sup>2</sup>
$T/H$	Thrust - horsepower ratio
$V$	Velocity, ft/sec
$W$	Slot height, ft
$w/C$	Slot height - chord ratio
$x$	Dimensionless radius, $r/R$
$\bar{X}$	Drag of internal obstruction

#### GREEK SYMBOLS

$\alpha$	Section angle of attack, deg
$\beta$	Blade twist, deg
$\delta$	Section camber
$\gamma$	Ratio of specific heats, (1.4)
$\theta_c$	Collective pitch, deg
$\rho$	Density, lb-sec <sup>2</sup> /ft <sup>4</sup>
$\sigma$	Rotor solidity, $\frac{NC}{\pi R}$
$\bar{\Omega}$	Rotational velocity vector, rad/sec
$\eta_c$	Compressor efficiency (assumed 0.8)
$\phi_i$	Induced angle, deg

### Subscripts

ATM	Atmospheric conditions
C	Compressor
COR	Coriolis or pumping
d	Duct
I	Induced
J	Jet
P	Profile
TE	Trailing edge
T	Total
—	Average or mean quantities
O	Total conditions of flow

## INTRODUCTION

This paper examines the hover performance of a four-bladed high speed rotor of constant chord, zero twist, and varying sectional properties. Although it had been determined previously (Reference 1) that an ideal Circulation Control (CC) rotor could generate Figures of Merit approaching 0.90, it was not known what performance degradation would be incurred with a more practical configuration. In particular, the effect of tip Mach number, collective pitch, zero twist, and slot height variation were unknown so that the present investigation was needed.

The theoretical and experimental performance of blown rotor systems such as the blown flap, jet flap and circulation control have been under investigation for many years (References 2 thru 7). These systems generally enhanced the aerodynamic capabilities of the helicopter in such areas as speed, propulsive force, lift capability, stability and control, and vibratory stress control. However, almost without exception the power requirements to achieve these improvements were excessive so that the overall vehicle performance was marginal.

Recently a new generation of circulation control airfoils has been developed (References 8 to 21). These airfoils exhibit greatly improved aerodynamic efficiency at higher lift coefficients so that the rotor efficiency is similarly improved. Although the full performance potential of this new rotor system has yet to be established, present computations (Reference 12) indicate nominally a factor of two increases in cruise speed and efficiency over conventional rotors.

The extension to higher cruise capability of any V/STOL is in direct conflict with good hover efficiency. In general a compromise of blade twist, solidity, and section properties is necessitated to afford an equitable tradeoff. The circulation control rotor essentially circumvents the hover-cruise compromise by efficiently controlling blade lift distribution independent of twist (angle of attack), and solidity (chord). By minimizing the solidity and completely eliminating the twist, a rotor-borne speed potential of approximately 400 knots is possible at rotor lift to equivalent drag rotors on the order of 20.0 (Reference 12).

The original hover methodology described in Reference 8, has undergone several refinements principally in the area of section aerodynamics, induced velocity and internal flow calculations. The new analysis will therefore be described in some detail before discussing the calculation results.

#### HOVER METHODOLOGY

Hover performance for a selected thrust is computed by a series of successive iterations on the hub plenum pressure, internal duct losses and the induced velocity. Figure 1 shows a logic diagram of the computer program.

The program inputs include the rotor geometry and operating conditions. The Lock-Goldstein vortex method is used to calculate the inflow field. A one-dimensional compressible flow analysis computes the internal blade duct pressure and temperature variation for a given compressor pressure ratio. The local radial variation of momentum coefficient is computed from the duct flow variables and the specified slot height distribution. Detailed airfoil section characteristics are employed to calculate the elemental forces and moments at each radial station. Finally these variables are integrated to yield rotor thrust and power. If the thrust is not sufficient the compressor pressure ratio is increased until the specified level is reached. The induced velocity is iterated upon within this loop.

The following sections discuss the performance computations in more detail.

#### TOTAL POWER COMPUTATION

The power required for a circulation controlled rotor consists of four components:

$$P_T = P_I + P_{COR} + P_C + P_P \quad (1)$$

where  $P_I$  is the induced power

$P_{COR}$  is the coriolis or pumping power

$P_C$  is the compressor power (including duct losses)

$P_P$  is the profile power

The hovering efficiency or Figure of Merit is given in terms of the ratio of the minimum theoretical induced power to the total power required by the rotor.

$$FM = \frac{P_{I_{min}}}{P_T} = \frac{0.707 C_T^{3/2}}{C_P} \quad (2)$$

This parameter may be used to compare with other rotors in hover. Each of the power terms will be discussed in the following sections.

#### INDUCED POWER

The method of Lock-Goldstein is employed for the calculation of the induced velocity field and the induced power (Reference 22). This is a modified vortex theory which assumes a noncontracting wake of distributed vorticity from a specified number of blades having an arbitrary span loading distribution. It is highly suitable for performance calculation as it requires minimal computer time while eliminating the empirical "tip correction factors" of other theories. Although not the ultimate vortex theory, the method is quite accurate in the range of conventional rotor thrust coefficients. However, with increasing thrust coefficient or increasing numbers of blades the Lock-Goldstein method becomes progressively optimistic as indicated in Reference 23. This result is due primarily to the inherent assumption of a constant helix angle and noncontracting wake which does not adequately locate the position of the trailing vortex shed by a previous blade. In actuality the vortex from the preceding blade may remain in the rotor tip path plane (Reference 23) and pass only slightly under the following blade, thereby causing localized changes in angle of attack and high power consumption. On the other hand a jet sheet such as generated by a circulation control rotor can have two favorable influences on the tip vortex: (1) it may dissipate the concentrated vorticity and virtually eliminate the adverse tip effect (Reference 24) and (2) it may force the vortex (which acts as a free streamline) to move downward from the tip path plane. Furthermore, the more ideal span load distribution (discussed subsequently) should significantly reduce the tip loading and concentrated vorticity.

Very little information is currently available on the induced velocity field of a circulation control rotor with which a suitable theory might be developed. However, one series of tests have been conducted (in Reference 25) with which an approximate correction factor may be developed. Figure 2a shows the experimental rotor lift distribution of a twelve foot circulation control rotor ( $C_T/\sigma = 0.283$ ). The measured (pitot survey) induced velocity field immediately below the rotor is shown in Figure 2b including the calculated induced velocity using Lock-Goldstein between  $0.14 \leq X \leq 0.95$ . From  $X = 0.95$  to  $X = 1.00$  (tip), it is assumed that the induced velocity decays linearly to zero to match the experimental findings. The tip vortex impingement assumption effects the performance calculations by generating large angles of attack in that region which result in a significant increase in drag. At the same time any lift increment is excluded from the calculation.

The tip approximation is used throughout the analysis at considerably lower values of  $C_T/\sigma$  than that of Figure 2. It is therefore felt that the corrected Lock-Goldstein method is probably quite accurate for the range of  $C_T/\sigma \leq 0.28$ .

Using the assumptions described above the induced power is then calculated from:

$$P_I = \frac{N \rho R V_T^3}{2} \int_0^{1.0} x^3 C_L(x) C(x) \sin \phi_1(x) dx \quad (3)$$

#### CORIOLIS POWER (PUMPING POWER)

The radial airflow inside the duct induces a coriolis torque which must be added to the profile and induced torque. This torque can be derived as follows:

The tangential acceleration (normal to span axis) of a fluid particle moving out the blade radius is:  $\bar{a} = 2 \bar{\Omega} \times \bar{V}_d$ .

where  $\bar{\Omega}$  is the rotational velocity vector

and  $\bar{V}_d$  is the velocity vector of a small particle of fluid in the duct in the rotating system.

The differential force acting on a small mass of fluid,  $dm$ , normal to  $\bar{\Omega}$  and  $\bar{V}_d$  is therefore

$$|d\bar{F}| = 2 \Omega V_d dm \quad (4)$$

the torque is

$$dQ = r dF \quad (5)$$

A change of variables is next made by noting

$$V_d dm = \rho_d A V_d dr = \dot{m} dr \text{ or in terms of initial mass flow rate, } \dot{m}_T,$$

$$V_d dm = \left[ \dot{m}_T - \int_{R_1}^r \left( \frac{d\dot{m}}{ds} \right) ds \right] dr \quad (6)$$

This equation represents the mass flow rate of the air in the duct at any radial station and hence the coriolis power is given by

$$P_{COR} = \Omega Q = 2 \Omega r^2 \int_{R_1}^R r \left[ \dot{m}_T - \int_{R_1}^r \left( \frac{d\dot{m}}{ds} \right) ds \right] dr \quad (7)$$

It may be seen that this power varies with the initial mass flow rate and the distribution of mass flux radially. In general, coriolis power amounts to less than five percent of the total power in hover.

#### COMPRESSOR POWER AND DUCT LOSSES

The compressor power requirement is computed from the isentropic relation:

$$P_c = \frac{\dot{m}_T g \bar{R} \gamma T_{ATM} \left[ \left( P_o / P_{ATM} \right)^{\frac{\gamma-1}{\gamma}} - 1 \right]}{(\gamma - 1) \eta_c} \quad (8)$$

The unknowns in this equation are the mass flow rate  $\dot{m}_T$ , and the total pressure,  $P_0$ . The determination of these two parameters involves a complex calculation of the losses in the ducting system. This calculation is based on the one-dimensional compressible flow analysis due to Shapiro. Various special cases of the analysis have been conducted in the literature (References 26 and 27). However, it is thought that the following equations represent the first complete formulation of the distributed mass efflux problem of the CCR.

The duct flow is represented by a one-dimensional compressible flow model. Any deviations from this model due to coriolis accelerations in the plane of rotation or other effects (leading to possible secondary flows) are accounted for by the friction coefficient and recovery factor which are altered empirically in accord with the findings of several investigators (notably Reference 26 which gives a Coriolis correction). The flow may be laminar, transitional or fully developed although for all but very small model rotors it would probably be fully turbulent.

The analysis may be developed from first principles as given by Shapiro (Reference 27) and modified by Henry (Reference 28) for inclusion of the centrifugal compression terms. The distributed ejection as formulated by Shapiro is valid if it is assumed that the air leaves the duct with the same state properties as the duct air and if the coefficient of gas injection,  $y = -1.0$ .

The following governing equation may then be derived from momentum, continuity and state equations for the variation of the internal duct Mach number with radius due to the mass efflux, friction, centrifugal compression, area change, temperature distribution and internal obstructions:

$$\frac{dM}{dr} = \left[ \frac{\gamma M^3 \left(1 + \frac{\gamma-1}{2} M^2\right)}{(1 - M^2)} y + \frac{M (1 + \gamma M^2) \left(1 + \frac{\gamma-1}{2} M^2\right)}{(1 - M^2)} \right] \frac{1}{M} \frac{dm}{dr} \\ + \left[ \frac{2\gamma M^3 \left(1 + \frac{\gamma-1}{2} M^2\right)}{1 - M^2} \right] \frac{\bar{f}}{D} - \left[ \frac{M \left(1 + \frac{\gamma-1}{2} M^2\right)^2}{g (C_p - C_v) J T_T (1 - M^2)} \right] \Omega^2 r$$

$$\begin{aligned}
& - \left[ \frac{M (1 + \frac{\gamma-1}{2} M^2)}{(1 - M^2)} \right] A_d \frac{1}{dr} \frac{dA_d}{dr} + \left[ \frac{M (1 + \gamma M^2) (1 + \frac{\gamma-1}{2} M^2)}{2 (1 - M^2)} \right] \frac{1}{T_T} \frac{dT_T}{dr} \\
& + \left[ \frac{\gamma M^3 (1 + \frac{\gamma-1}{2} M^2)}{2 (1 - M^2)} \right] \frac{1}{\frac{\gamma}{2} P_d M^2 A_d} \frac{d\bar{X}}{dr}
\end{aligned} \tag{9}$$

To solve the equation independent expressions are needed for the variation of the slot height, duct internal area and internal obstructions and an auxiliary relation is required for the temperature variation. The temperature equation is derived from the energy equation and the Reynold's analogy to yield:

$$\frac{dT_T}{dr} = \frac{(\gamma-1) T_{ATM} M_T^2 r}{R} + \frac{2\bar{f}}{D} (T_w - T_{aw}) \tag{10}$$

To find the wall temperature,  $T_w$ , a relationship between the flow total temperature,  $T_T$ , and the heat transfer characteristics of the duct is also needed. This expression is:

$$\frac{T_w}{T_T} = 1 - k \left( 1 - \frac{T_{ATM}}{T_T} \right), \text{ where } 0 \leq k \leq 0.5 \tag{11}$$

A detailed calculation of  $k$  would depend on the thermal resistance of the blade material and on the convection cooling of the external surface. For the present study a value of  $k = 0.3$  is taken as representative of current technology. As the effects of heat transfer are quite small for the relatively low temperature flows considered herein their representation is entirely sufficient.

The duct flow equation is solved by a forward difference technique as follows: (1) The entry mass flow and duct Mach number are

estimated from the compressor pressure ratio and temperature. (2) Each term of Equation (9) is next estimated for a distance  $\Delta r$  down the duct, the Mach number at this station calculated and a new estimate made until a converged value is reached. (3) This process is repeated for up to 160 duct stations finally yielding the duct Mach number at the end. (4) For a closed end duct the Mach number must be zero so that if an excess exists the original entry estimate is reduced and the computation is repeated. (5) If the Mach number tends to zero before the end of the duct the original estimate is increased. Once the internal Mach number distribution is established the analysis computes the spanwise variations of duct pressure and blowing coefficient,  $C_\mu$ .

A typical duct loss computation is shown in Figure 3 for the present rotor assuming no internal obstructions and an internal duct area equal to the airfoil cross section. Due to the highly optimistic result (large total pressure rise), and because a realistic internal blade geometry (spars, turning vanes, etc.) was not yet available, it was decided to simply use the conservative assumption of constant duct pressure for the present performance calculations.

It should be noted, however, that these rather surprising results imply that a significant measure of control air can be provided simply by centrifugal pumping. This result may have important implications for autorotation or even an unaugmented air supply.

#### PROFILE POWER

The profile power is computed in the conventional manner,

$$P_P = \frac{N \rho R V_T^3}{2} \int_0^{1.0} C_d(x) C(x) x^3 \cos \phi_1(x) dx$$

where  $C_d(x)$  is a function of the section thickness-chord ratio, camber, angle of attack, blowing coefficient, slot height to trailing edge radius ratio, slot height to chord ratio and free-stream Mach number. The present analysis uses a cambered twenty percent thickness root section which tapers linearly to a symmetrical fifteen percent tip

section (Figure 4). The detailed airfoil data and compressibility factors are given in Appendix A.

## ROTOR GEOMETRY AND OPERATING CONDITIONS

The rotor (Figure 4) is described completely by the following dimensionless variables which are inputs to the analysis

$x$	Radial location, unit at tip
$C/R(x)$	Local chord-rotor radius ratio
$\beta(x)$	Twist, degrees
$\delta(x)$	Section camber
$t/C(x)$	Section thickness-chord ratio
$R_{TE}/C(x)$	Local trailing edge radius-chord ratio, immediately after slot exit
$w/C(x)$	Slot height-chord ratio
$N$	Number of blades

For the present study the following characteristics were used:

$C/R(x)$	$= 0.07$
$\beta(x)$	$= 0$
$\delta(x)$	$= (0.05 - 0.05X)$
$t/C(x)$	$= (0.20 - 0.05X)$
$R_{TE}/C(x)$	$= (0.04 + 0.064X)$
$W/C(x)$	$= 0.001; 0.002$
$N$	$= 4$
$\sigma$	$= 0.082$
$\eta_c$	$= 0.80$

The range of operational variables investigated consisted of the following:

$$0.0025 \leq C_T \leq 0.020$$

$$0.51 \leq M_{TIP} \leq 0.91$$

$$0.0 \leq P_{duct}/P_{atm} \leq 1.8$$

$$0.0 \leq \theta_C \leq 16.0^\circ$$

Sea level standard conditions were assumed.

## RESULTS

Three parameters were varied in the present study: collective pitch, slot height and tip Mach number. Each of these is discussed below in the context of optimum Figure of Merit. The results are then summarized in terms of the dimensional power loading and disc loading and compared with a conventional rotor.

### EFFECT OF COLLECTIVE PITCH

Figure 5 shows the typical effect of varying collective pitch at constant values of rotor thrust coefficient. At a nominal design value of thrust coefficient ( $C_T = 0.010$ ) a collective pitch setting of approximately nine degrees would yield the maximum hover efficiency.

The breakdown of hover power components is shown in Figure 6 for the  $C_T = 0.010$  case. It may be noted that the induced power is generally close to the ideal, differing by about six percent at the minimum total power point. The reason for this relatively efficient induced power requirement may be noted in Figures 7 and 8 where the radial loading and induced velocity distributions are shown. In general at the smaller collective pitch angles the distributions are close to the ideal illustrating that the circulation control rotor can achieve near optimum span loading with a constant slot height distribution ( $w/C = 0.001$ ).

A second important feature which can be noted in Figure 6 is that the contribution of the remaining power terms,  $C_{P_E}$  is approximately twenty three percent. This is somewhat less than the analogous profile power of a conventional rotor and is due primarily to the extremely low compressor power requirement (approximately four percent of total). Some further insight into this somewhat surprising result may be gained from Figure 9 where the primary duct flow variables are presented. Due to the high lift augmentation, the required mass flow is extremely low, with duct pressures amounting to about 2 psig at the maximum efficiency point.

### EFFECT OF SLOT HEIGHT

Two constant blade slot height to chord ratios were examined in the study,  $w/C = 0.001$ , and  $0.002$ . The larger slot height was preferable for the high speed cruise condition as it would permit the same momentum

flux ( $C_\mu$ ) to be obtained at a lower compressor power. The experimental airfoil data utilized is for  $w/c = 0.00125$  and it can be shown (References 13 and 14) that this value adequately represents the lift and drag characteristics for the two slot height ratios selected. A slight improvement in the section efficiency occurs at the larger slot height ratio due to a reduction of the compressor power. It is important to note that beyond the  $w/c = 0.002$ , the airfoil aerodynamic characteristics change significantly and require the use of a new momentum coefficient which properly accounts for larger slot height variations (Reference 13).

The effect of slot height ratio is shown in Figure 10. The curves presented are the loci of maximum efficiency at each collective pitch setting. It may be seen that as anticipated from the two-dimensional characteristics the larger slot height ratio shows a slight increase in Figure of Merit.

#### EFFECT OF TIP MACH NUMBER

The effect of tip Mach number is shown in Figure 11. It may be noted that a favorable compressibility effect occurs for  $M_{tip} \leq 0.70$ .

At  $M_{TIP} = 0.80$  a gradual profile drag rise occurs, slight affecting the performance and at  $M_{TIP} = 0.90$  a large degradation occurs and the rotor lift is limited to lower thrust coefficients. Figure of Merit is still quite good even at the high Mach numbers. This phenomena is due to several interrelated compressibility effects which are discussed in Reference 13. The primary effect however is the inherent ability of a circulation control airfoil to obtain a higher critical Mach number than a conventional airfoil developing the same lift.

The associated collective pitch variation curves for three values of tip Mach number are presented in Figure 12.

#### EFFECT OF TIP MACH NUMBER AND DISC LOADING ON POWER LOADING

A useful dimensional method for comparing rotors of equal solidity is the variation of power loading  $T/\rho$ , with disc loading  $T/S$ . These parameters are defined in terms of the previous dimensionless variables as follows:

$$T/S = \rho V_T^2 C_T$$

$$T/P = \frac{550 \sqrt{2} \text{ FM}}{V_T C_T^{\frac{1}{2}}}$$

In Figure 13 the preceding results are replotted in terms of the above variables. For reference a conventional rotor blade of the same solidity and -5 degree twist is presented in Figure 14. This rotor was designed for a high speed (300 - 350 knot) compound helicopter (Reference 28) and is therefore a representative comparison.

It may be noted by reference to Figure 14 and the preceding figures that the circulation control rotor affords the aircraft designer a considerable latitude over the conventional rotor in the choice of hover tip speed, disc loading, and rotor solidity without incurring serious hover power penalties. It should be noted that the calculation does not include any air flow losses before the rotor head but does assume a compressor efficiency of eighty percent.

#### CONCLUSIONS

1. A refined method of hover analysis has been presented for the calculation of circulation control airfoil performance. This method is believed to yield good accuracy within the limits specified.
2. A four-bladed, constant chord, untwisted circulation control rotor can achieve rotor Figures of Merit of 0.80 at thrust coefficients of 0.020.
3. A positive blade collective pitch angle is desirable to achieve high efficiency in hover. For a given design thrust range a single collective angle is adequate.
4. Tip Mach number has a favorable influence on the hover efficiency up to 0.70.

5. The hover power loading characteristics of a high speed circulation control rotor are superior to a conventional high speed rotor in the range of practical disk loadings.

Aviation and Surface Effects Department  
Naval Ship Research and Development Center  
Bethesda, Maryland 20034  
August 1971

#### ACKNOWLEDGEMENT

The author would like to express appreciation to Messrs. Ettore Mori, Joseph B. Wilkerson, and Drew W. Linck for their assistance in developing the computer program; Harvey J. Howe for assisting in the duct loss analysis; and to Ernest O. Rogers and Rodney C. Hemmerly for programming assistance.

## APPENDIX A

### SECTION DATA

The analysis employs experimental airfoil data for the root and tip sections and interpolates linearly in between. The root section is a twenty percent thickness ratio ellipse with five percent circular camber and a four percent circular trailing edge radius. The tip section is a fifteen percent symmetrical ellipse with an elliptical trailing edge. Figure 4 shows these sections and Figures A1 - A4 present the airfoil characteristics as used in the computerized format. The section data (lift and drag coefficient) is given in an incompressible form for a full angle of attack range.

Limited data (Reference 10) was also available for determining compressibility effect. This information was put into the form of a compressibility correction factor,  $F$ , given as a function of the slot height to local trailing edge radius ratio ( $W/R_{TE} = (W/C)/(R_{TE}/C)$ ), the momentum coefficient ( $C_\mu$ ) and free-stream Mach number. The development of this correction factor is given in Reference 13.

The effect of compressibility on the lift at any given section is then determined as:  $C_{l,compress.}(M, \alpha, C_\mu, t/c, \delta, W/R_{TE}) = F C_{l,Incompress.}(\alpha, C_\mu, t/c, \delta)$  where  $F$  is the ratio of compressible to incompressible lift coefficient and is functionally dependent on the free-stream Mach number ( $M$ ), blowing coefficient ( $C_\mu$ ), and slot height-trailing edge radius ratio ( $W/R_{TE}$ ).

In this manner the effect on lift of varying the ratio of slot height to trailing edge radius between the root and tip may be determined and the approximate effect of compressibility on angle of attack, thickness and camber are also calculated. The lift compressibility factor  $F$  is shown in Figure A5a for the circular trailing edge and in Figure A5b for the elliptical trailing edge. It may be noted that a strong degradation of lift performance occurs in the circular case while a significant increase of lift occurs with the more elliptical case.

The drag data is treated in a similar manner to the lift for the two  $W/R_{TE}$  values (Figure A6).

## REFERENCES

1. Williams, Robert M. and Rodney A. Hemmerly. "Determination of the (Ideal Practical) Hover Efficiency of Circulation Control Rotors." Wash. Aug 1971, 40 p. incl. illus. (Naval Ship Research and Development Center, Tech Note AL-212)
2. Dorand, R. "The Application of the Jet-Flap to Helicopter Rotor Control." Journal Helicopter Association of Great Britain, Vol. 13, Dec 1949, p. 323
3. Kretz, Marcel and Dubus Clauda. "Research Study of a High Speed Helicopter Using the DH 2011 Jet-Flapped Rotor, U. S. Army European Res. Office (APO NY 09757) Contr. No. DA-91-591-EUC-3318-3660. Dorand Rpt DH.2011-A-E3, Jan 1967. 122 p. incl. illus.
4. McCloud, John L. III, W. T. Evans and James C. Biggers. "Performance Characteristics of a Jet Flap Rotor." NASA SP-116 Conf. on V/STOL Aircraft, Ames Res. Ctr. Apr 4-5, 1966
5. Greenman, R. N. and M. G. Gaffney. "Application of Circulation Control to Helicopters." Office of Naval Research Contract. Nonr 2197(00) Report No. ARD 158, 1957
6. Cheeseman, I. C. and A. R. Seed. "The Application of Circulation Control by Blowing to Helicopters." J.R. AE. S. July 1966
7. Smith, M. C. G. "The Aerodynamics of a Circulation-Controlled Rotor." Paper in 3rd CAL/AVLABS Symposium on Aerodynamics of Rotary Wing Aircraft. Buffalo. 18-20 June 1969
8. Williams, Robert M. "Some Research on Rotor Circulation Control." CAL/AVLABS Symposium on Aerodynamics of Rotary Wing and C/STOL Aircraft 3rd. Buffalo, June 1969, Proceedings v. 2.
9. Williams, Robert M. and Harvey J. Howe. "Two-Dimensional Subsonic Wind Tunnel Tests on a 20 Percent Thick, 5 Percent Cambered Circulation Control Airfoil." Wash. Aug 1970, 23 p. incl. illus. (Naval Ship Research and Development Center. Tech Note AL-176)

10. Englar, Robert J. "Two-Dimensional Transonic Wind Tunnel Tests of Three 15 Percent Thick Circulation Control Airfoils." Wash. Dec 1970. 70 p. incl. illus. (Naval Ship Research and Development Center. Tech Note AL-182)
11. Englar, Robert J. "Two-Dimensional Subsonic Wind Tunnel Tests on Two 15 Percent Thick Circulation Control Airfoils." Wash. Aug 1971. 56 p. incl. illus. (Naval Ship Research and Development Center. Tech Note AL-211)
12. Williams, Robert M. "Analysis of the Cruise Performance of a High Speed Circulation Control Rotor." (Naval Ship Research and Development Center. Tech Note AL- ) (to be published)
13. Williams, Robert M. "Design Considerations of Circulation Control Airfoils." (Naval Ship Research and Development Center. Tech Note AL-185) (In preparation)
14. Englar, Robert J. "Two-Dimensional Subsonic Wind Tunnel Tests of a Cambered 30 Percent Thick, Circulation Control Airfoil." (Naval Ship Research and Development Center. Tech Note AL- ) (to be published)
15. Williams, Robert M. and Kenneth R. Reader. "Two-Dimensional Subsonic Wind Tunnel Tests on a 50 Percent Thick Circulation Control Airfoil With Blowing Slots at 88.6 and 98.5 Percent Chord. (Naval Ship Research and Development Center. Tech Note AL-186) (In preparation)
16. Kind, R. J. and D. J. Maull. "An Experimental Investigation of a Low-Speed Circulation Controlled Airfoil." Aeronautical Quarterly, Vol. XIX, p. 170-182, May 1968
17. Kind, R. J. "A Calculation Method for Circulation Control by Tangential Blowing Around a Bluff Trailing Edge." Aeronautical Quarterly, Vol. XIX, p. 205-223, Aug 1968
18. Kind, R. J. "A Proposed Method of Circulation Control." PH.D. Dissertation, University of Cambridge, 1967

19. Kind, R. J. "Calculation of the Normal-Stress Distribution in a Curved Wall Jet." West Virginia University, Aerospace Engineering TR-18, Aug 1969
20. Ambrosiani, J. P. and N. Ness. "Analysis of a Circulation Controlled Elliptical Airfoil." West Virginia University, Aerospace Engineering TR-30, Apr 1971
21. Jones, D. G. "The Performance of Circulation-Controlled Aerofoils." Ph.D. Dissertation, University of Cambridge, July 1970
22. Lock, C. N. H. "The Application of Goldstein's Theory to the Practical Design of Airscrews, British ARC, R & M No. 1377, Nov 1930
23. Jenney, D. S., J. R. Olson and A. J. Landgrebe. "A Reassessment of Rotor Hovering Performance Prediction Methods. Journal of the American Helicopter Society, Vol. 13, No. 2, April 1968
24. Rinehart, Stephen A. "Study of Modification of Rotor Tip Vortex by Aerodynamic Means." Rochester Applied Science Interim Rpt. 70-02, 50 p. incl. illus. Jan 1970
25. Seed, A. R. Rotor Induced Flow Paper in AGARD No. 22, Sept 1967, Gottingen.
26. Kannamuller, G. "Efficiency Improvement of Helicopter Tip-Drive Systems." Paper No. 11 in AGARD Conference Proceedings No. 31, Jun 1968, Ottawa, Canada
27. Shapiro, Ascher H. and W. R. Hawthorne. "The Mechanics and Thermodynamics of Steady One-Dimensional Gas Flow." Journal of Applied Mechanics. Dec 1947, Vol. 14, No. 4, p. A-317
28. Henry, J. R. "One-Dimensional, Compressible, Viscous Flow Relations Applicable to Flow in a Ducted Helicopter Blade." NACA TN-3089, Dec 1953
29. Cruz, E. S., N. B. Govenberg, and A. W. Kerr. "A Flight Envelope Expansion Study for the XH-51A Compound Helicopter, USAAVLABS TR 69-78, Oct 1969, 109 p. incl. illus.

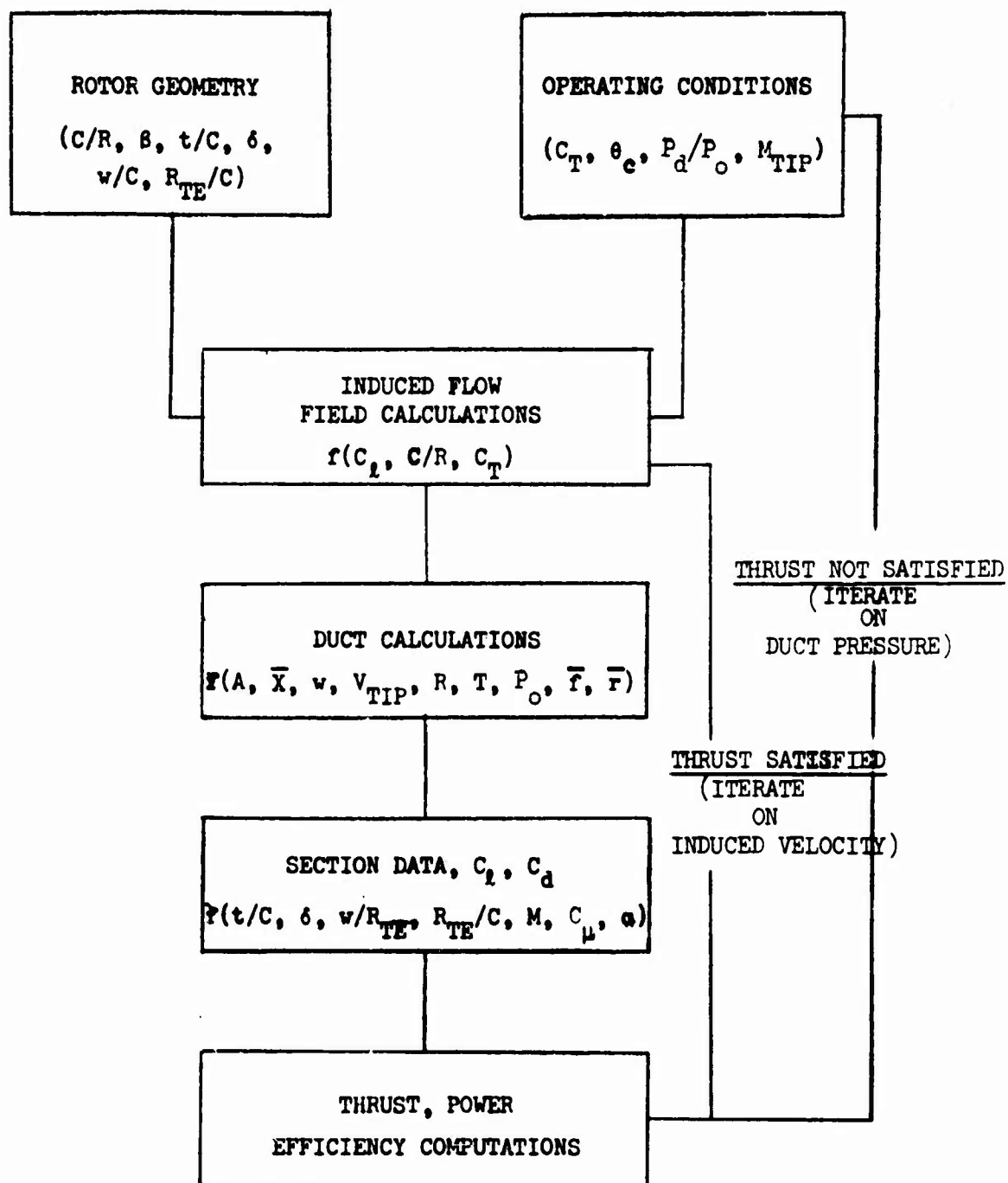
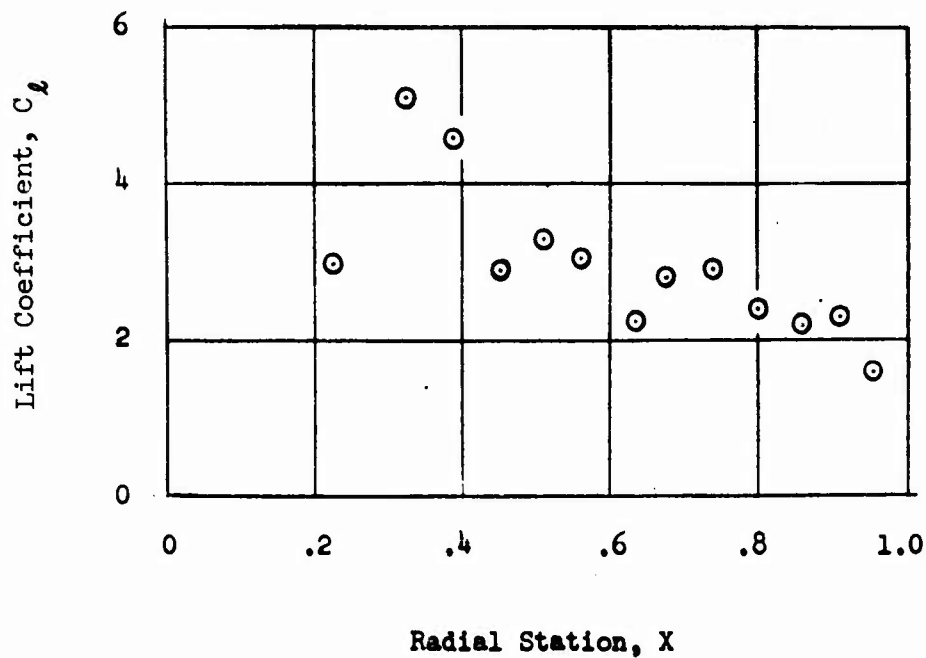
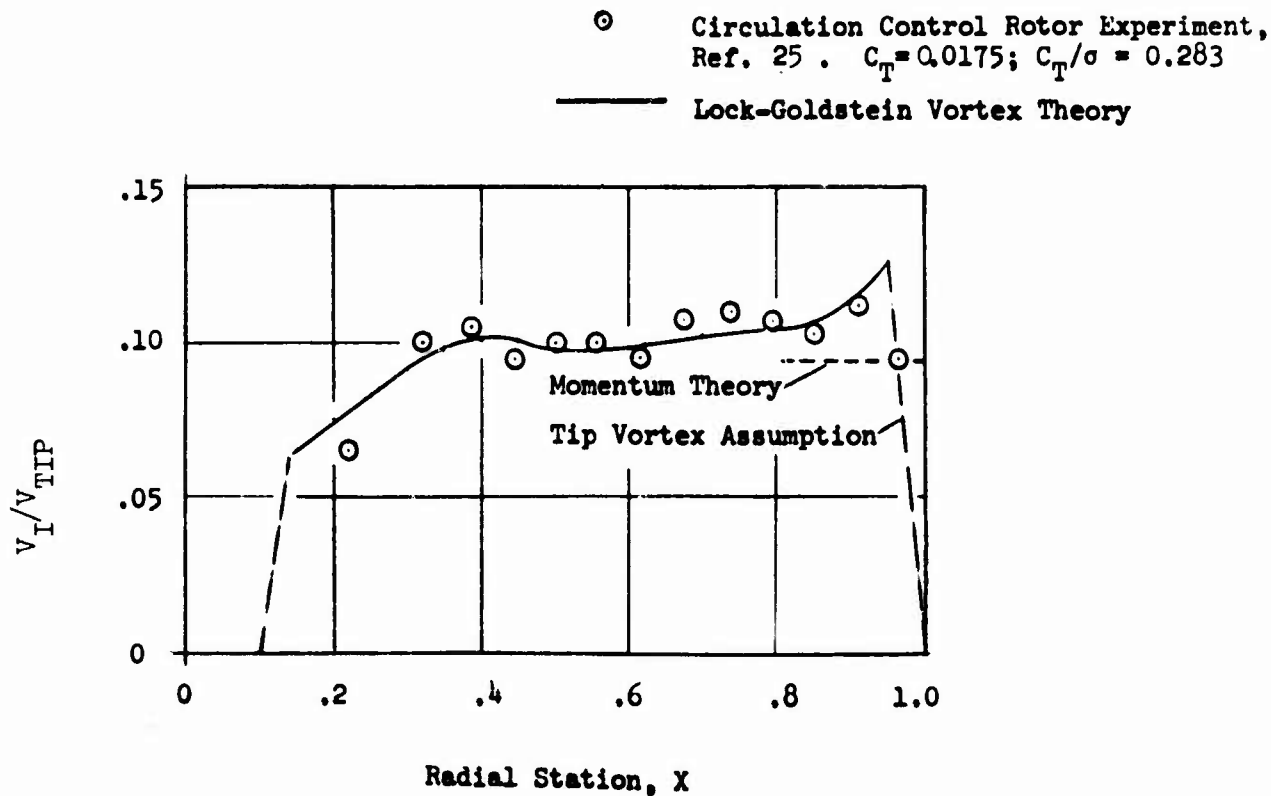


Figure 1 - Hover Methodology



(a) Lift Coefficient Versus Radial Station



(b) Inflow Ratio Versus Radial Station

Figure 2 - Comparison of Experiment with Lock-Goldstein Inflow Theory

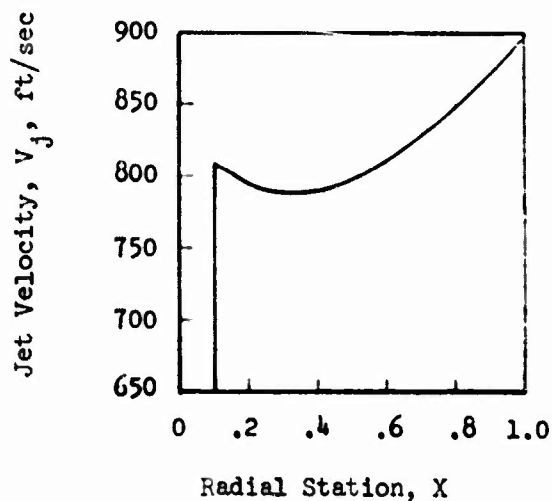
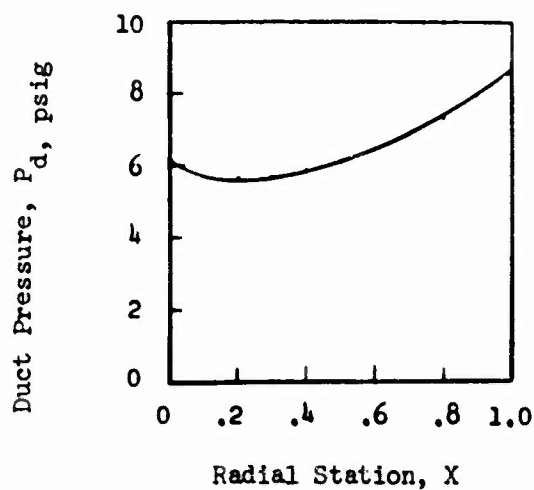
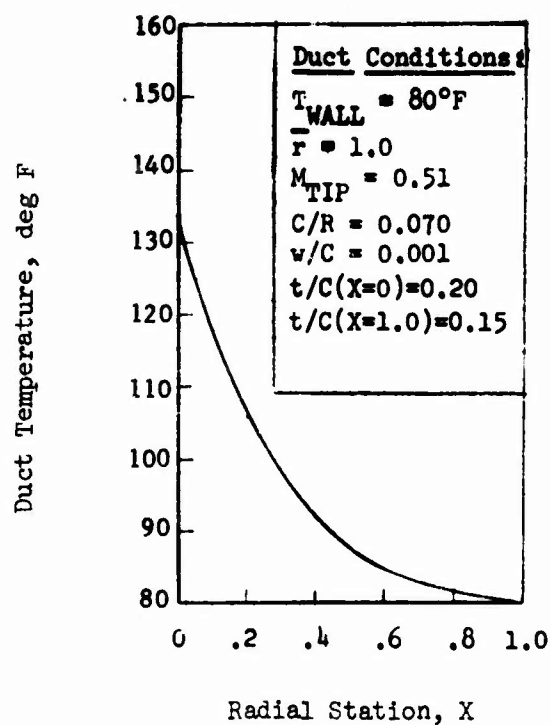
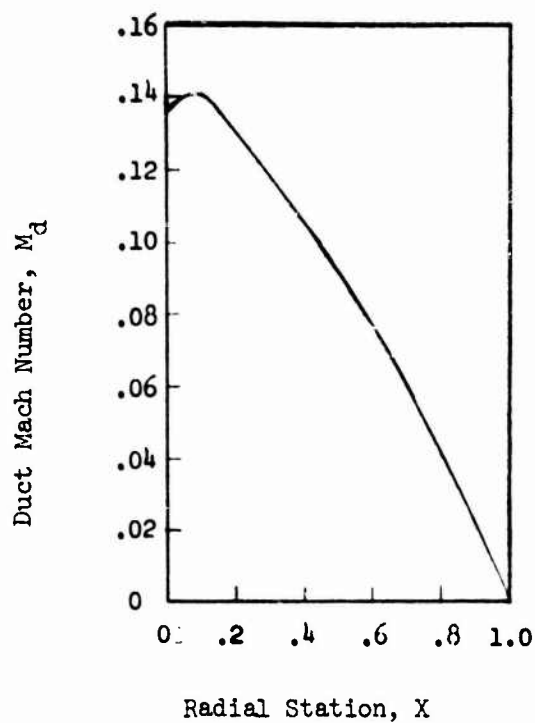
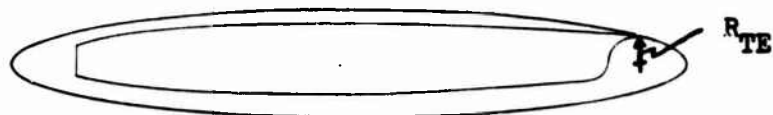
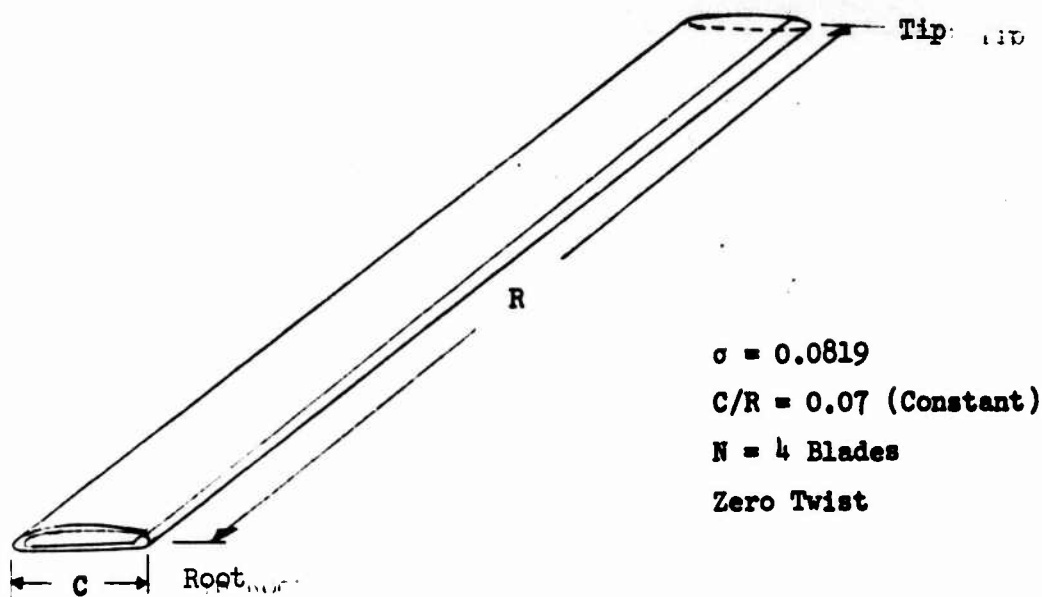


Figure 3 - Typical Radial Variation of Internal Flow  
Parameters in an Elliptical Cross Section Duct



Tip Section,  $t/C = 0.15$ ,  $\delta = 0$ .  
 Slot Position: 92.3% Chord



Root Section,  $t/C = 0.20$ ,  $\delta = 0.05$   
 Slot Position: 96.6% Chord

Figure 4 - Rotor Geometry

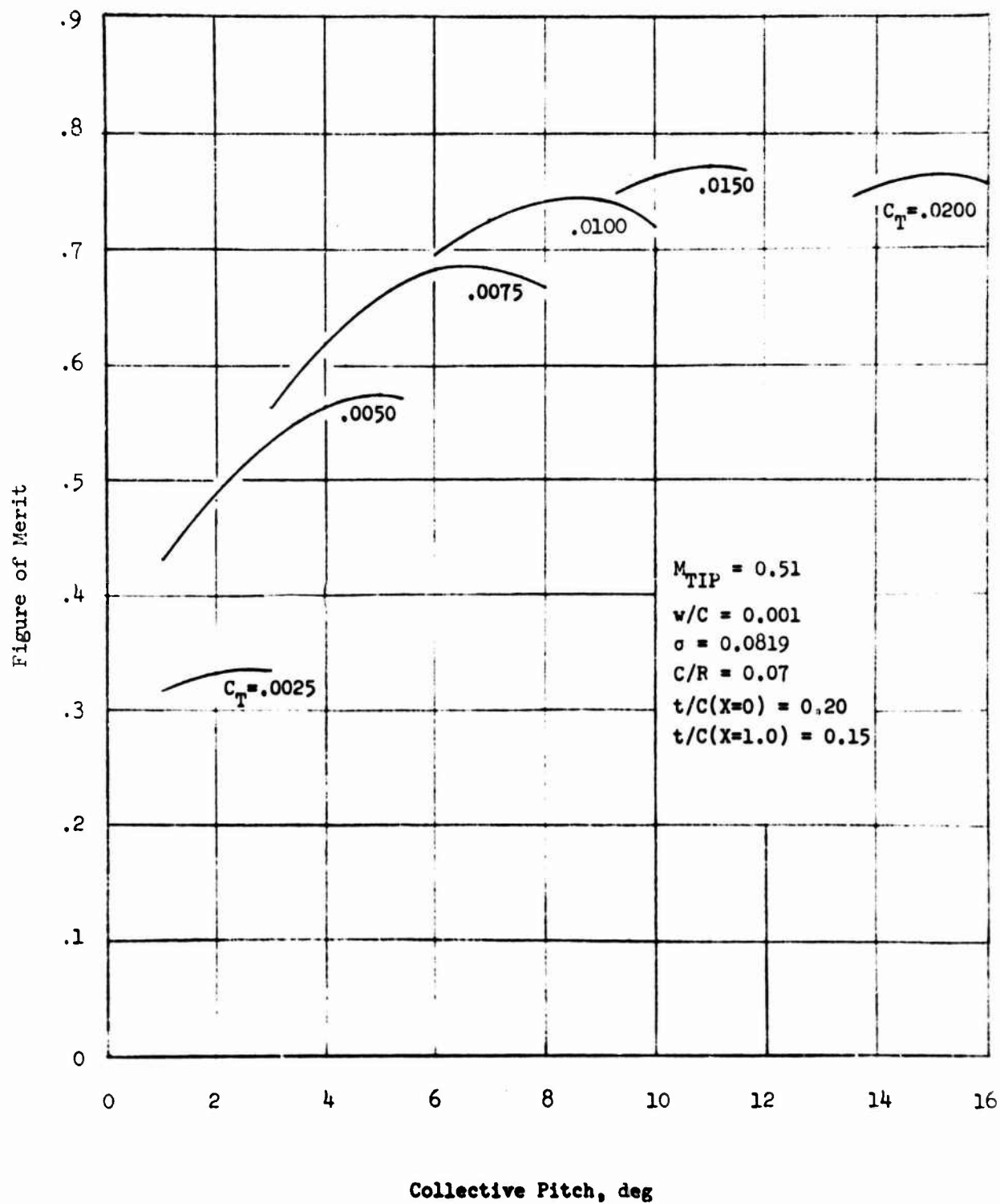


Figure 5 - Variation of Hover Figure of Merit with Collective Pitch and Thrust Coefficient

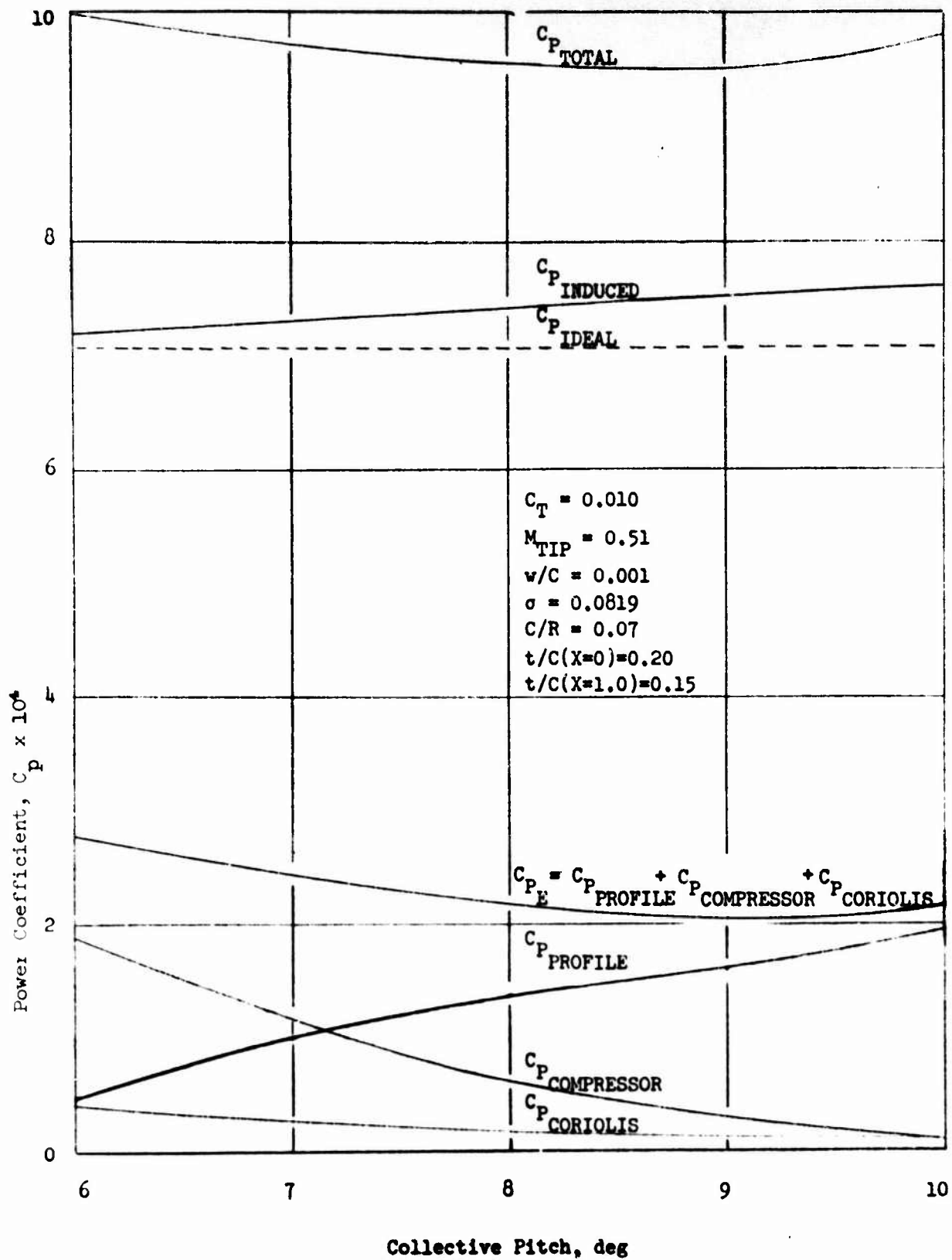


Figure 6 - Variation of Power Components with  
Collective Pitch,  $C_T = 0.010$

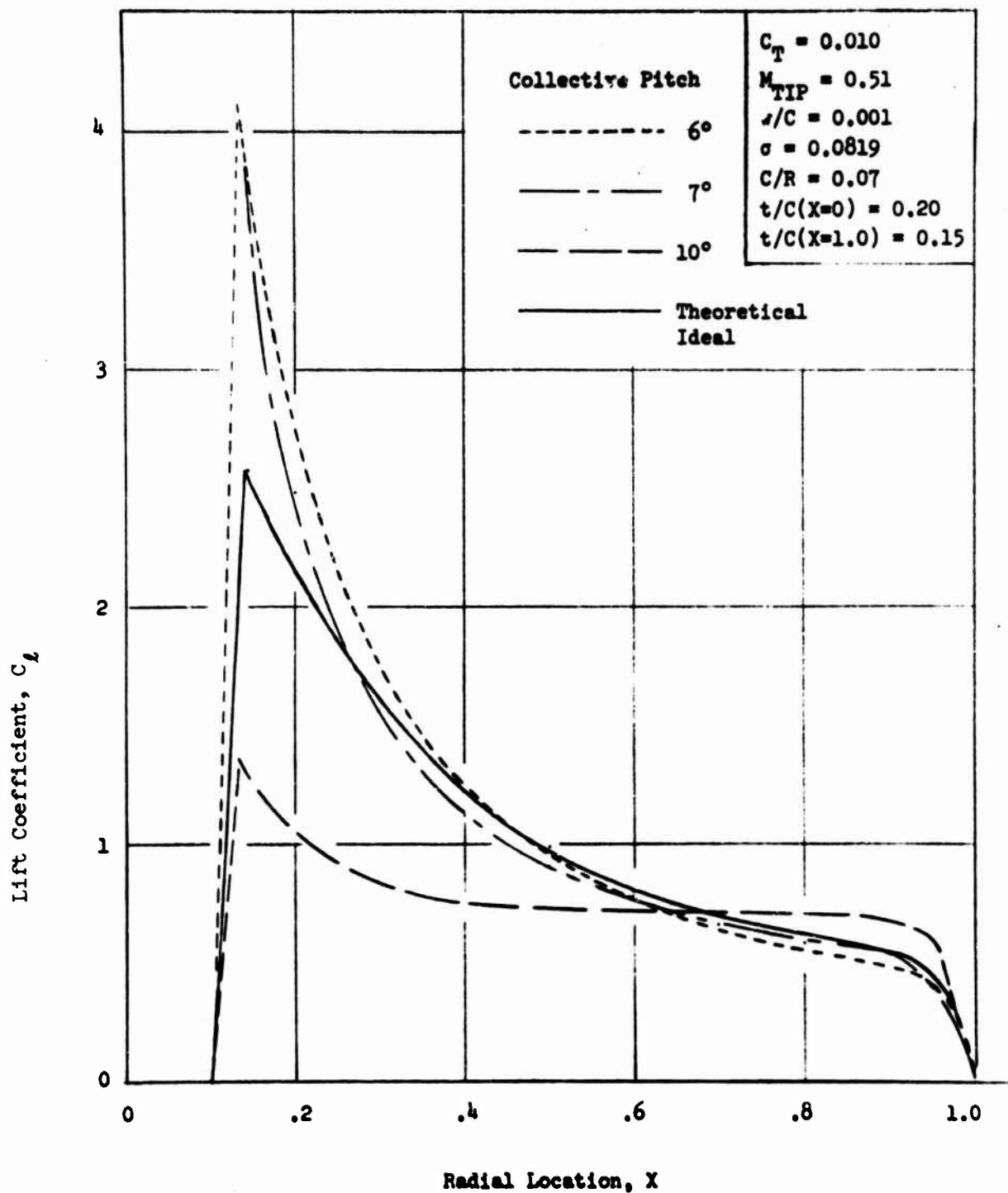


Figure 7 - Variation of Radial Load Distribution  
with Collective Pitch,  $C_T = 0.010$

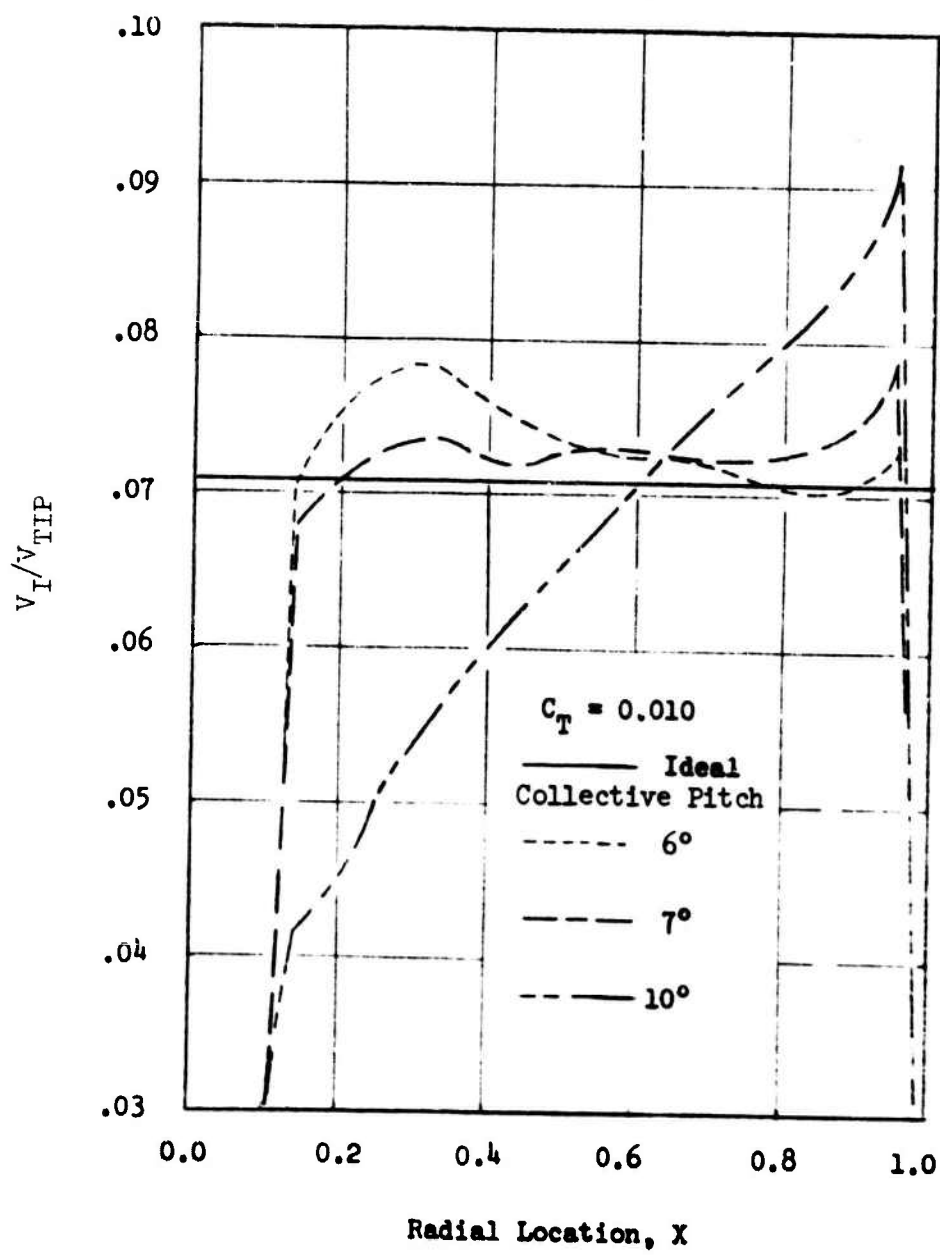
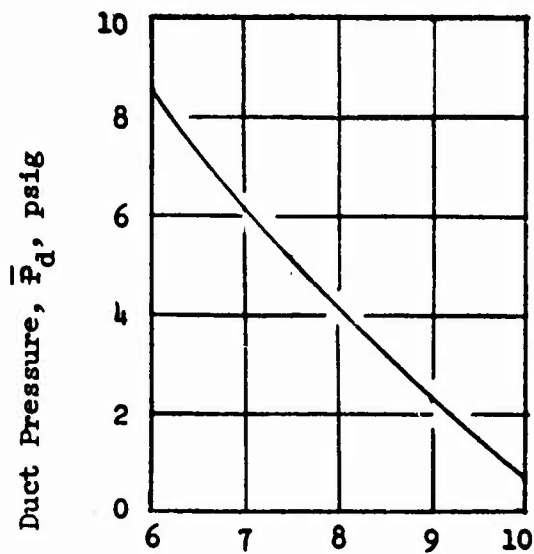
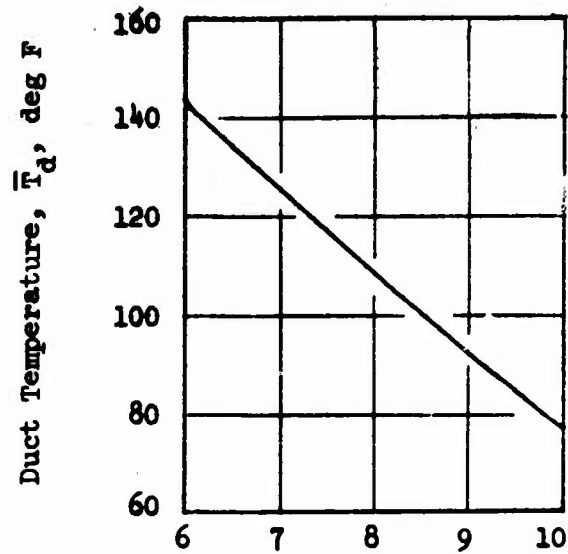


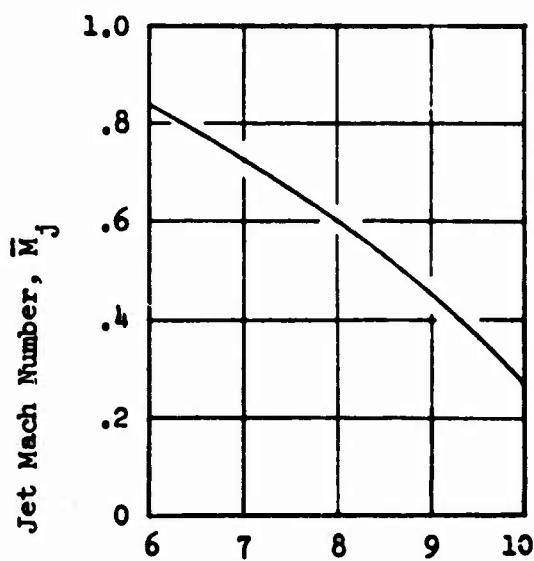
Figure 8 - Calculated Induced Velocity Distribution  
Corresponding to Lift Distributions of Figure 7



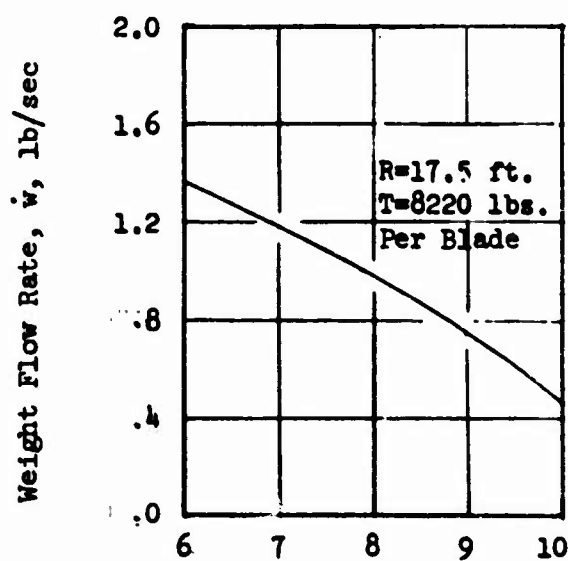
Collective pitch,  $\theta_c$ , deg



Collective pitch,  $\theta_c$ , deg



Collective pitch,  $\theta_c$ , deg



Collective pitch,  $\theta_c$ , deg

Figure 9 - Variation of Average Duct Flow Properties with Collective Pitch [For Rotor Parameters of Figures 5-8]

Figure of Merit

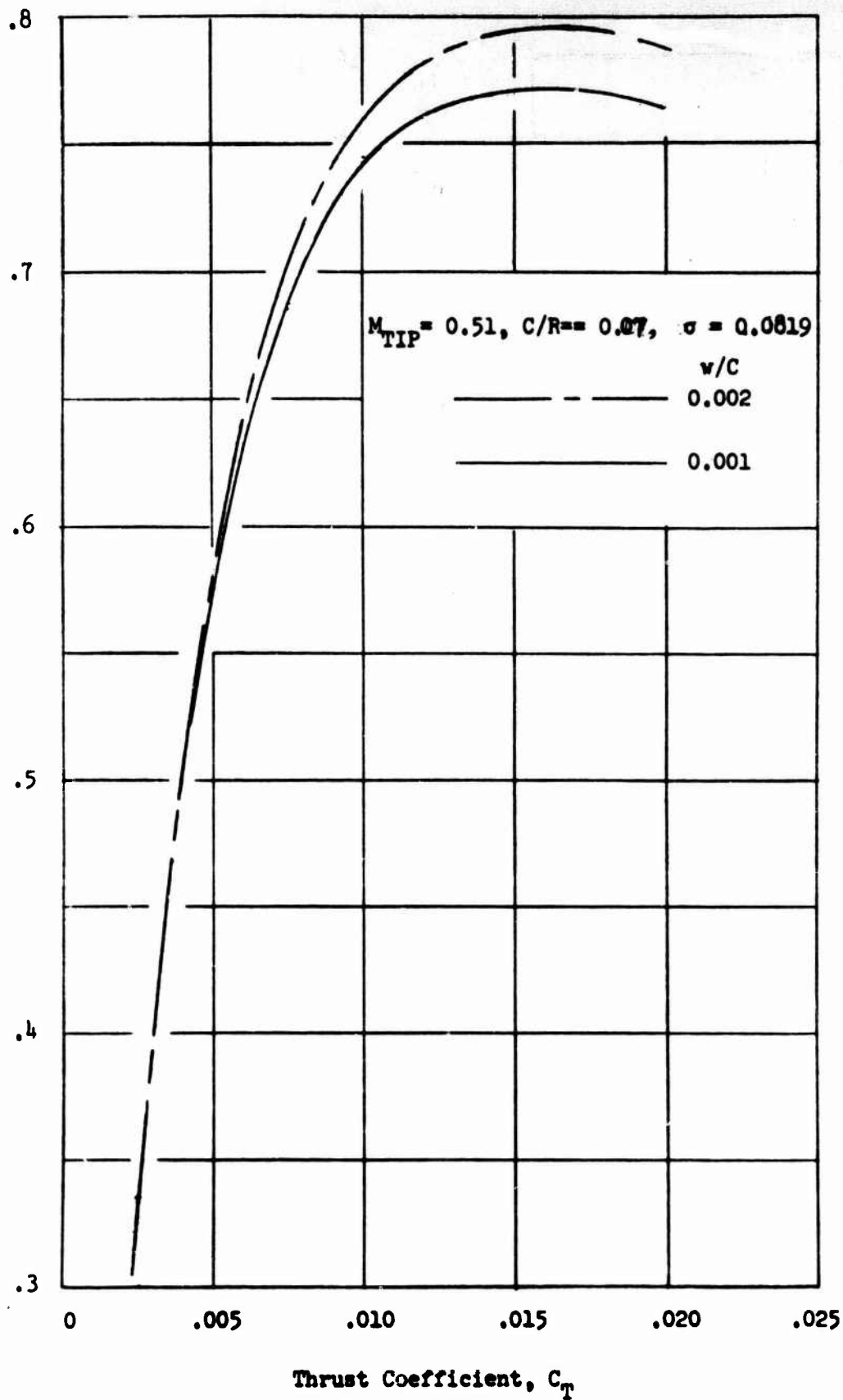


Figure 10 - Effect of Slot Height on Locus of Optimum Hover Figure of Merit

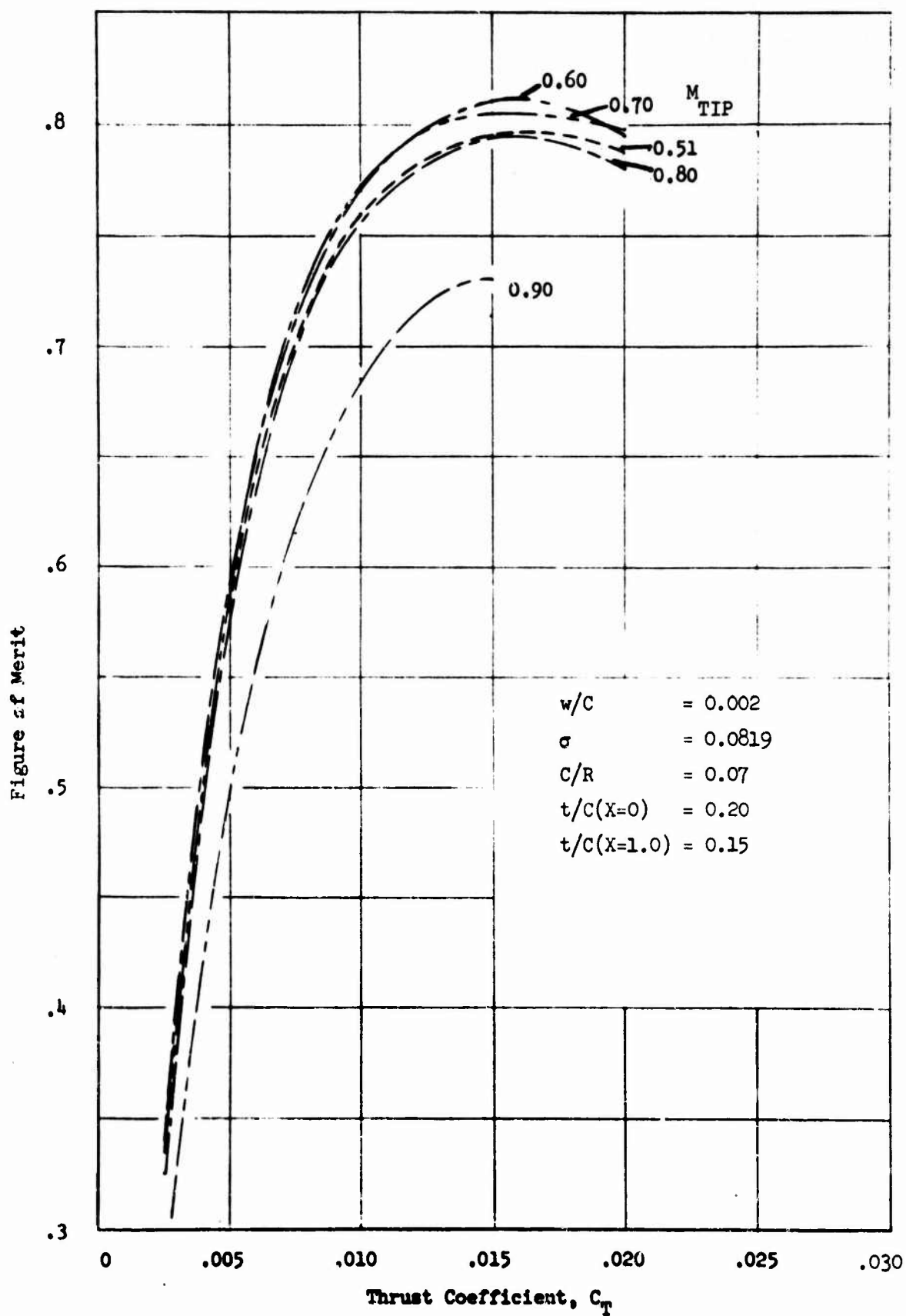


Figure 11 - Effect of Tip Mach Number on Figure of Merit

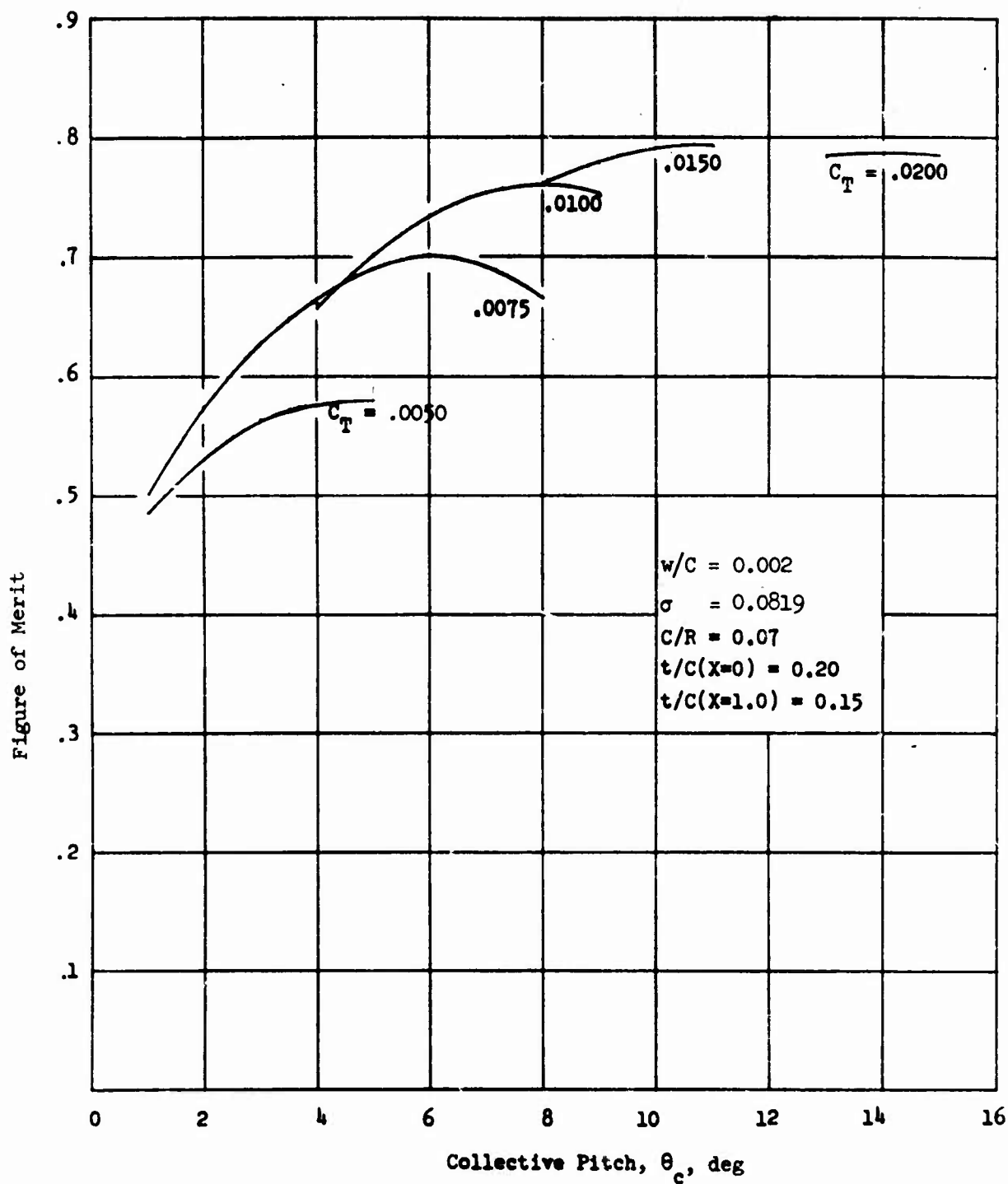


Figure 12 - Variation of Figure of Merit With Collective Pitch

(a)  $M_{TIP} = 0.51$

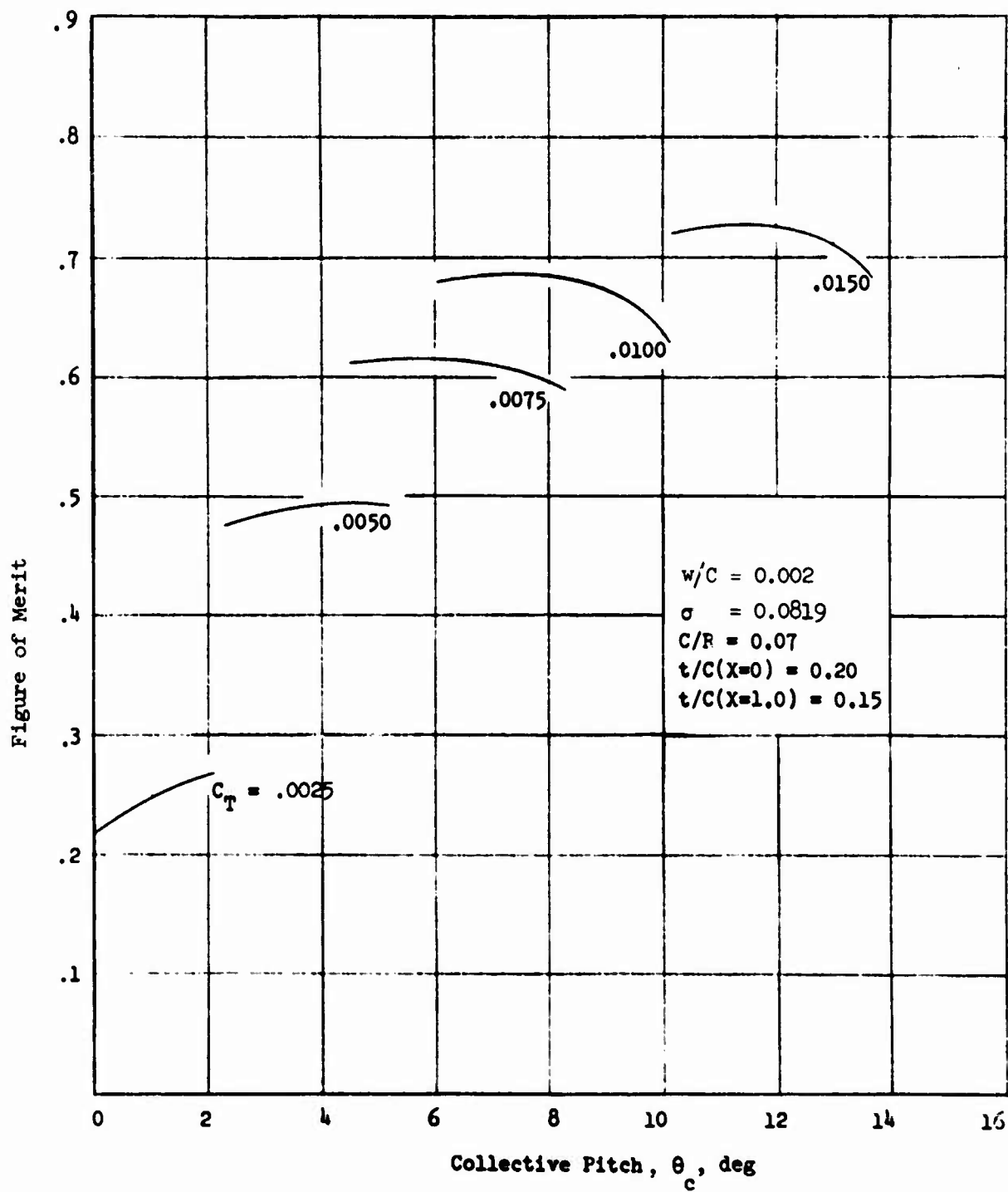


Figure 12 - (Cont.)

(c)  $M_{TIP} = 0.90$

Figure of Merit

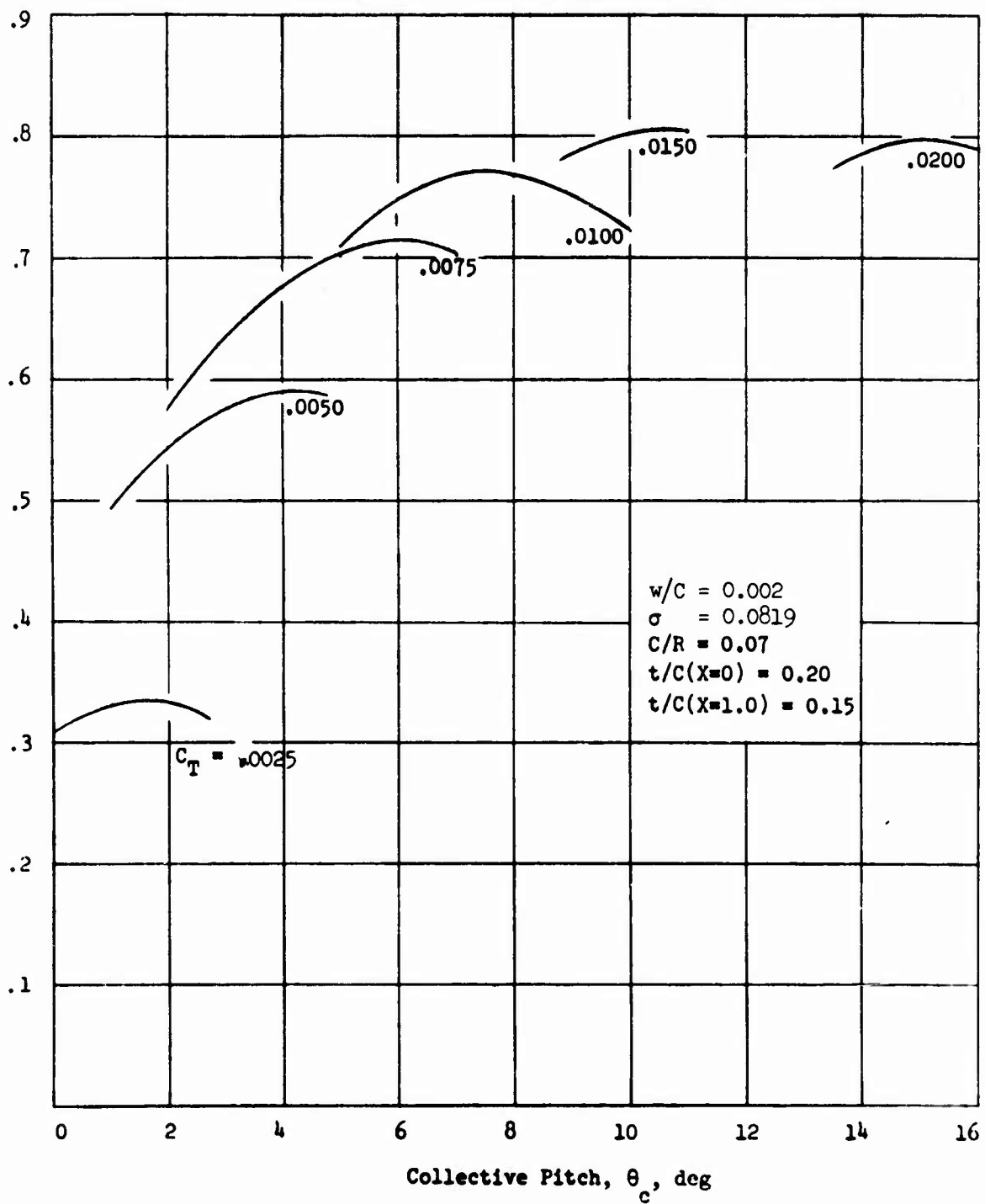


Figure 12 - (Cont.)

(b)  $M_{TIP} = 0.70$

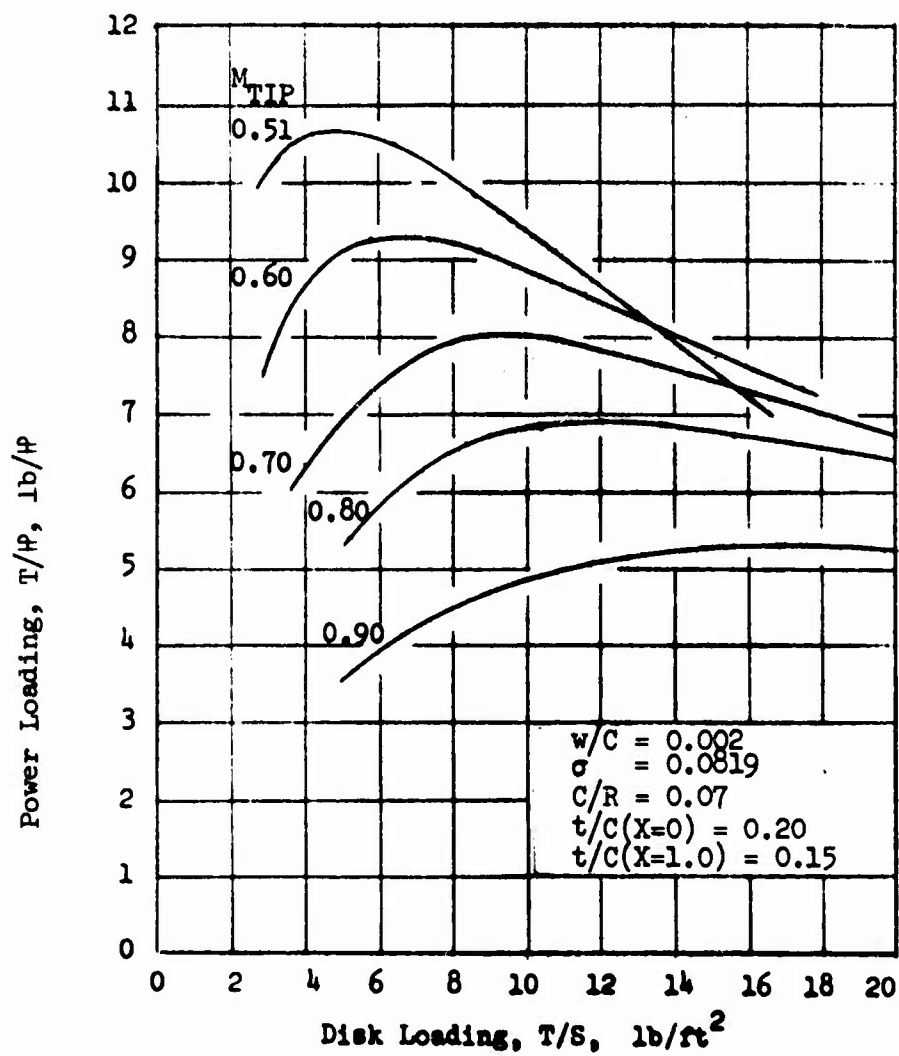


Figure 13 - Variation of Power Loading with Disc Loading and Tip Mach Number

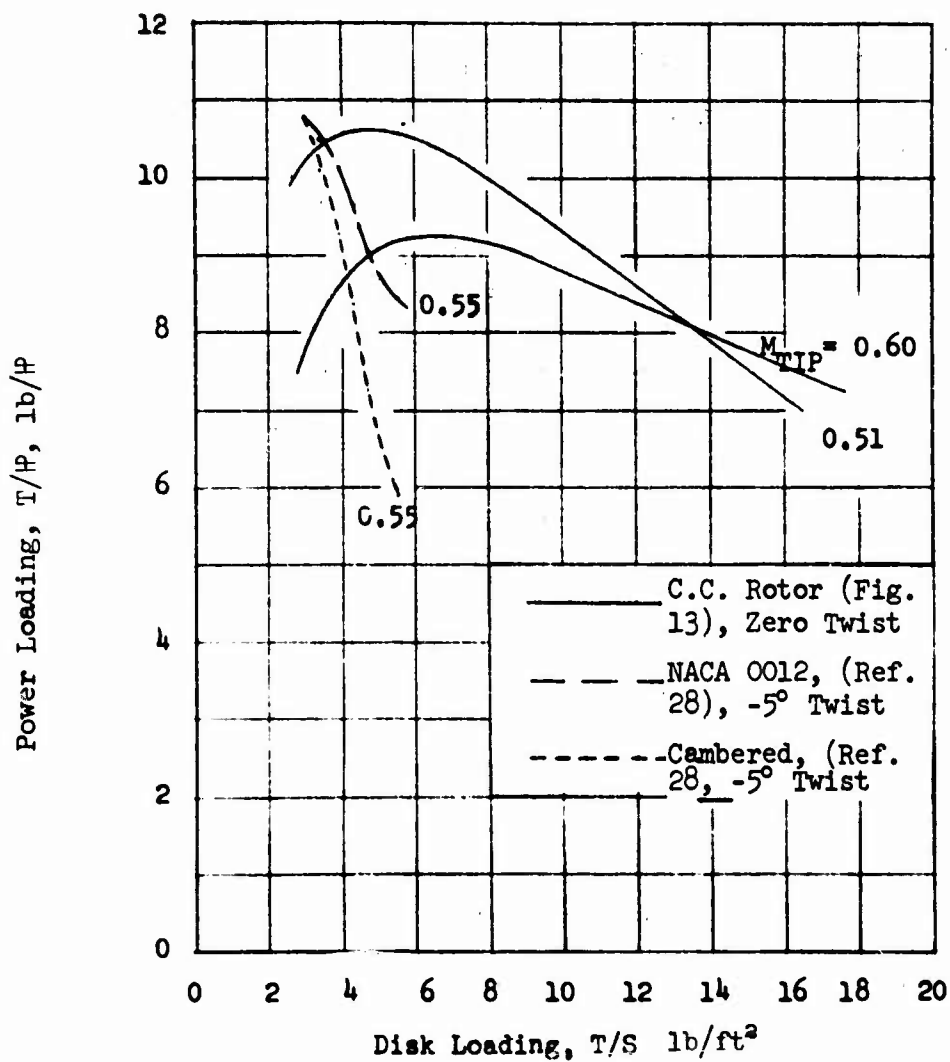


Figure 14 - Comparison of Circulation Control Rotor and High Performance Conventional Rotors of Same Solidity, ( $\sigma = 0.0819$ )

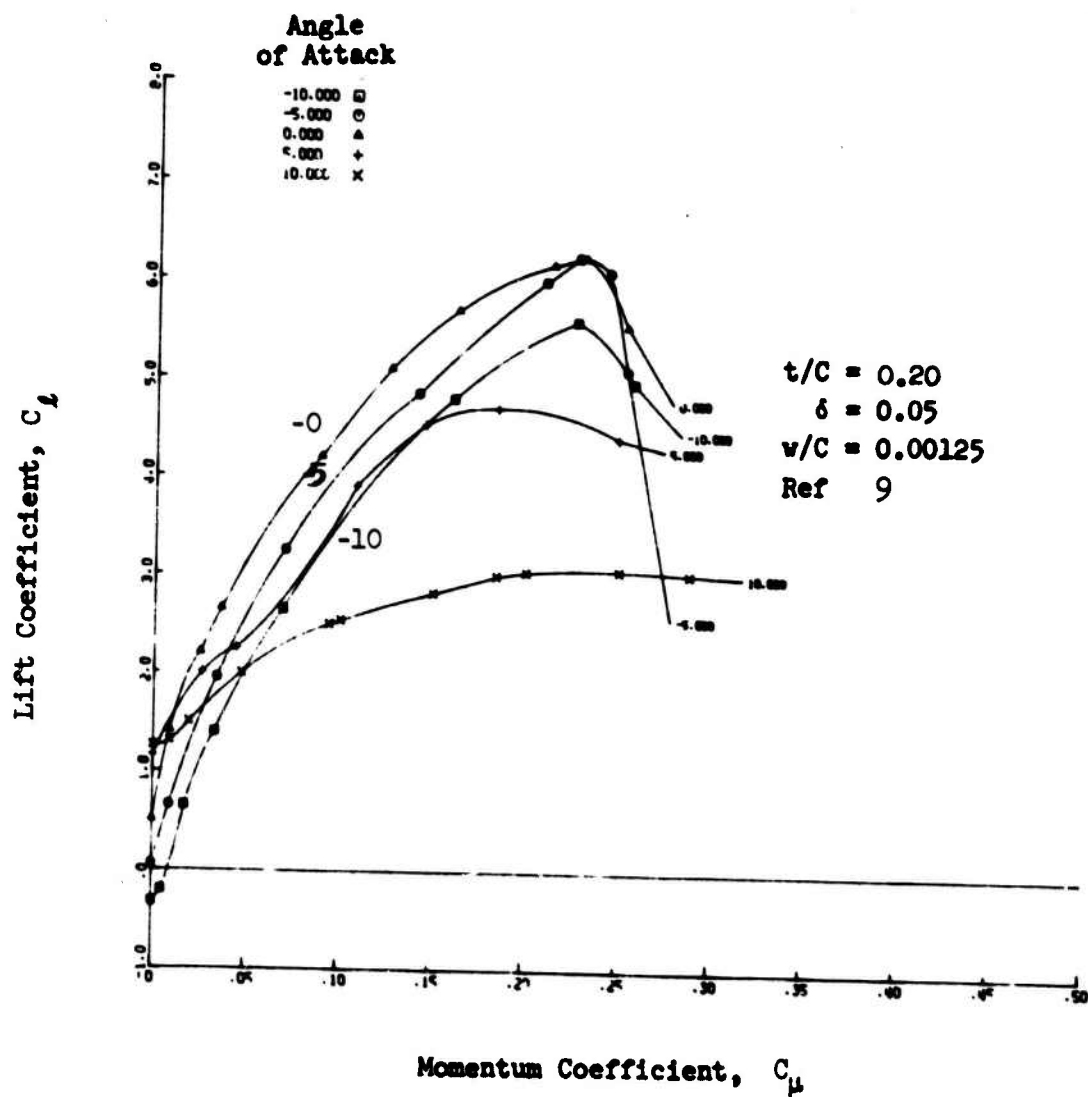


Figure A1 - Root Section Lift Characteristics

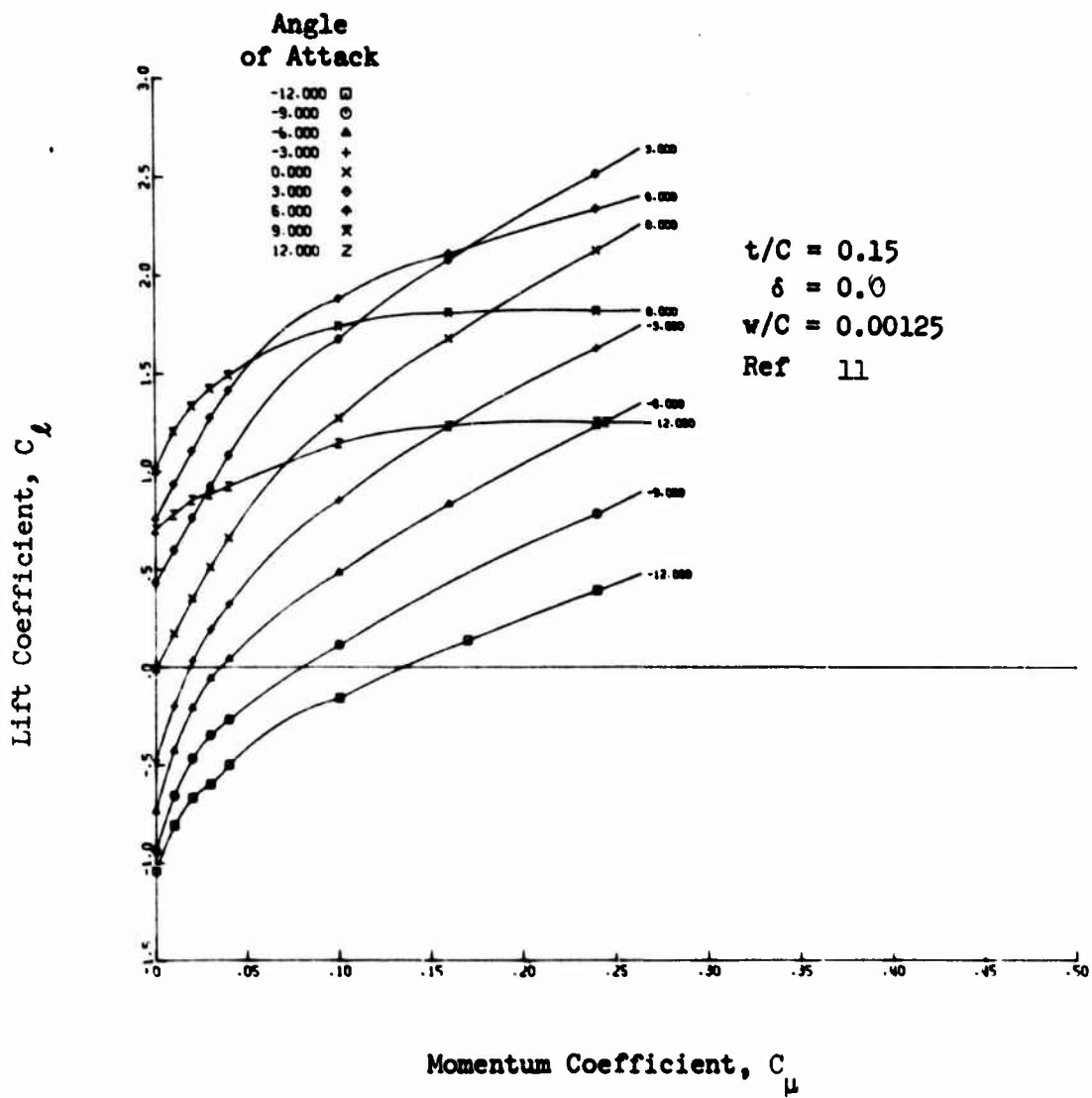


Figure A2 - Tip Section Lift Characteristics

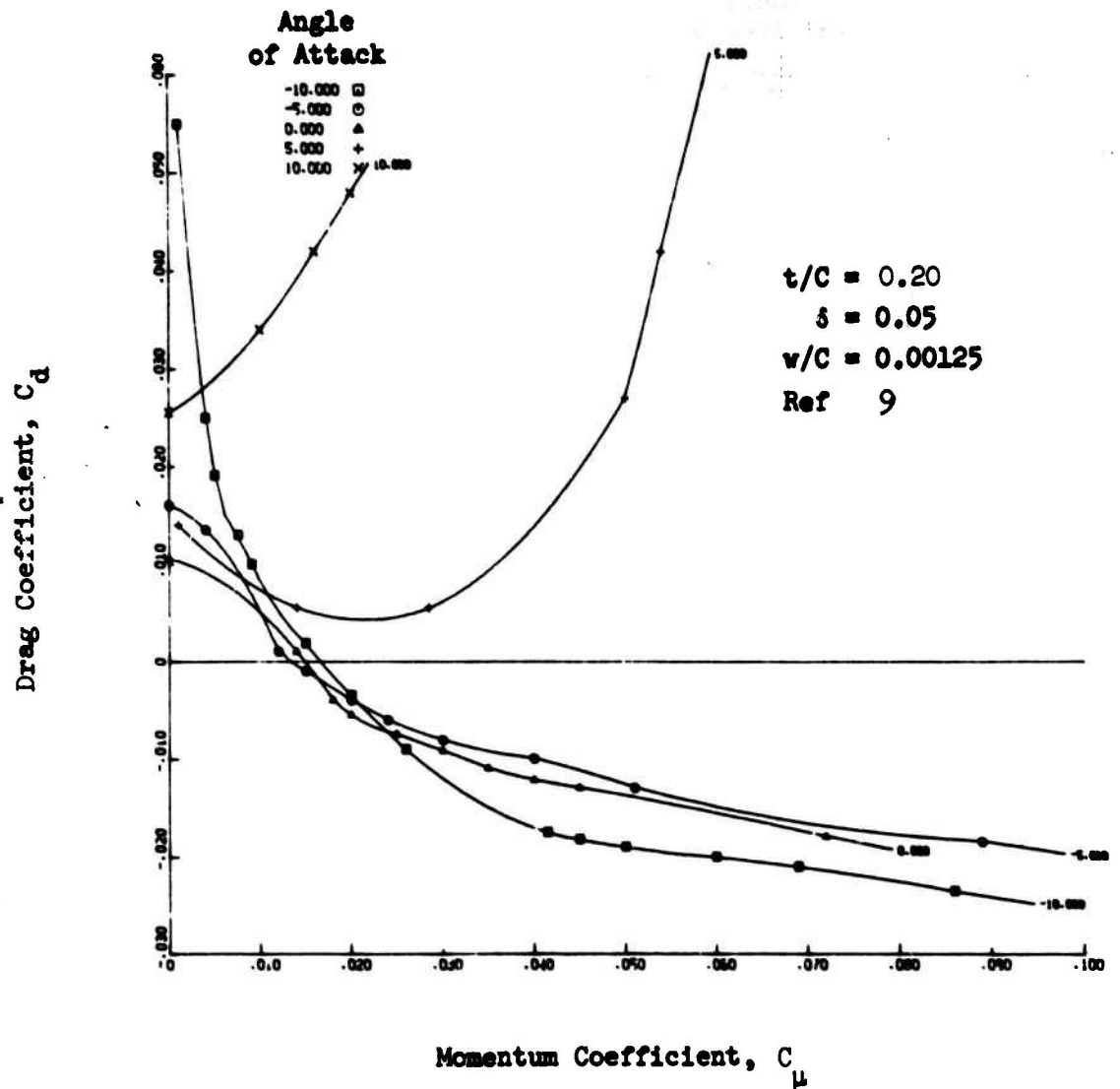
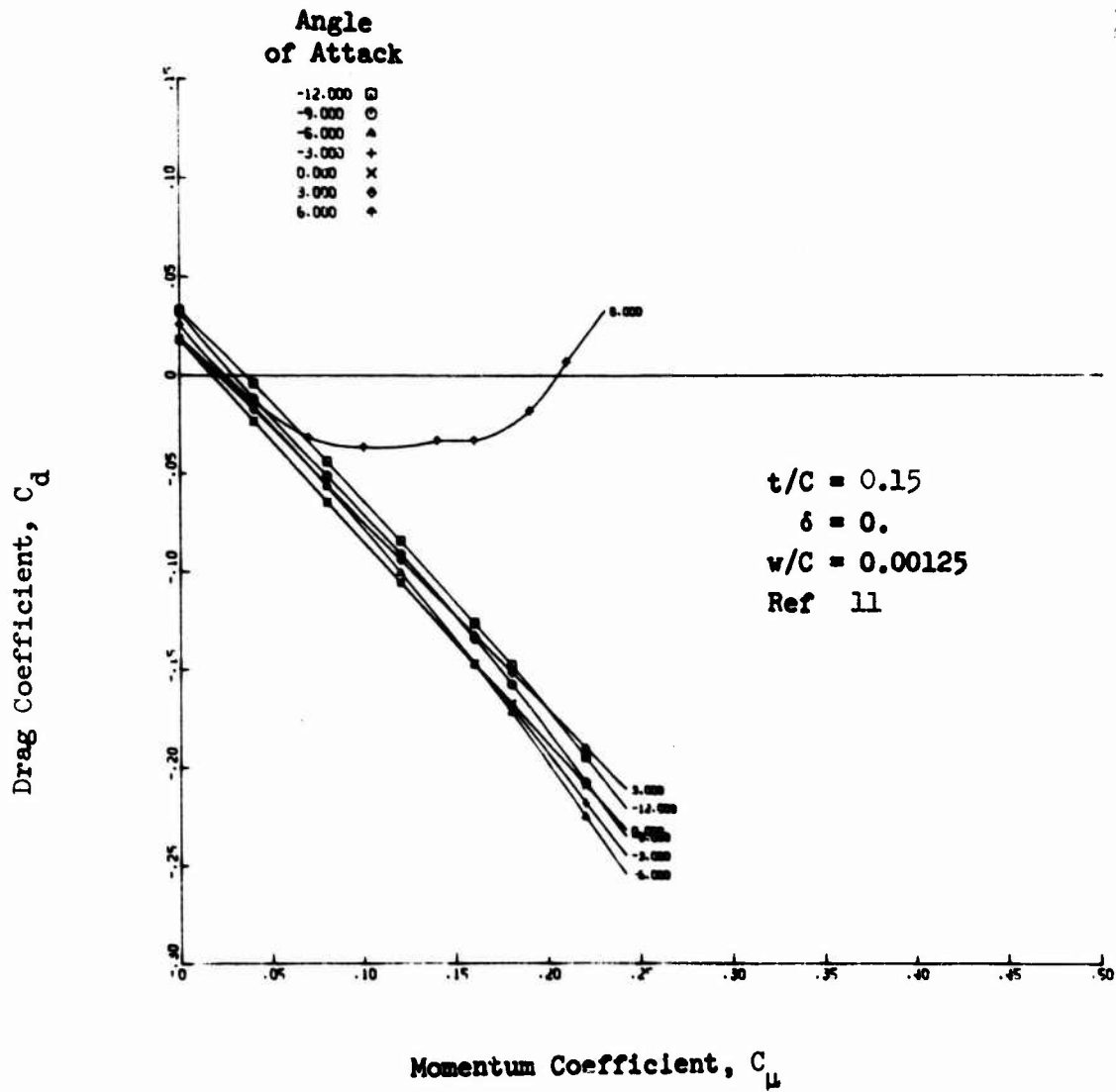


Figure A3 - Root Section Drag Characteristics



**Figure A4 - Tip Section Drag Characteristics**

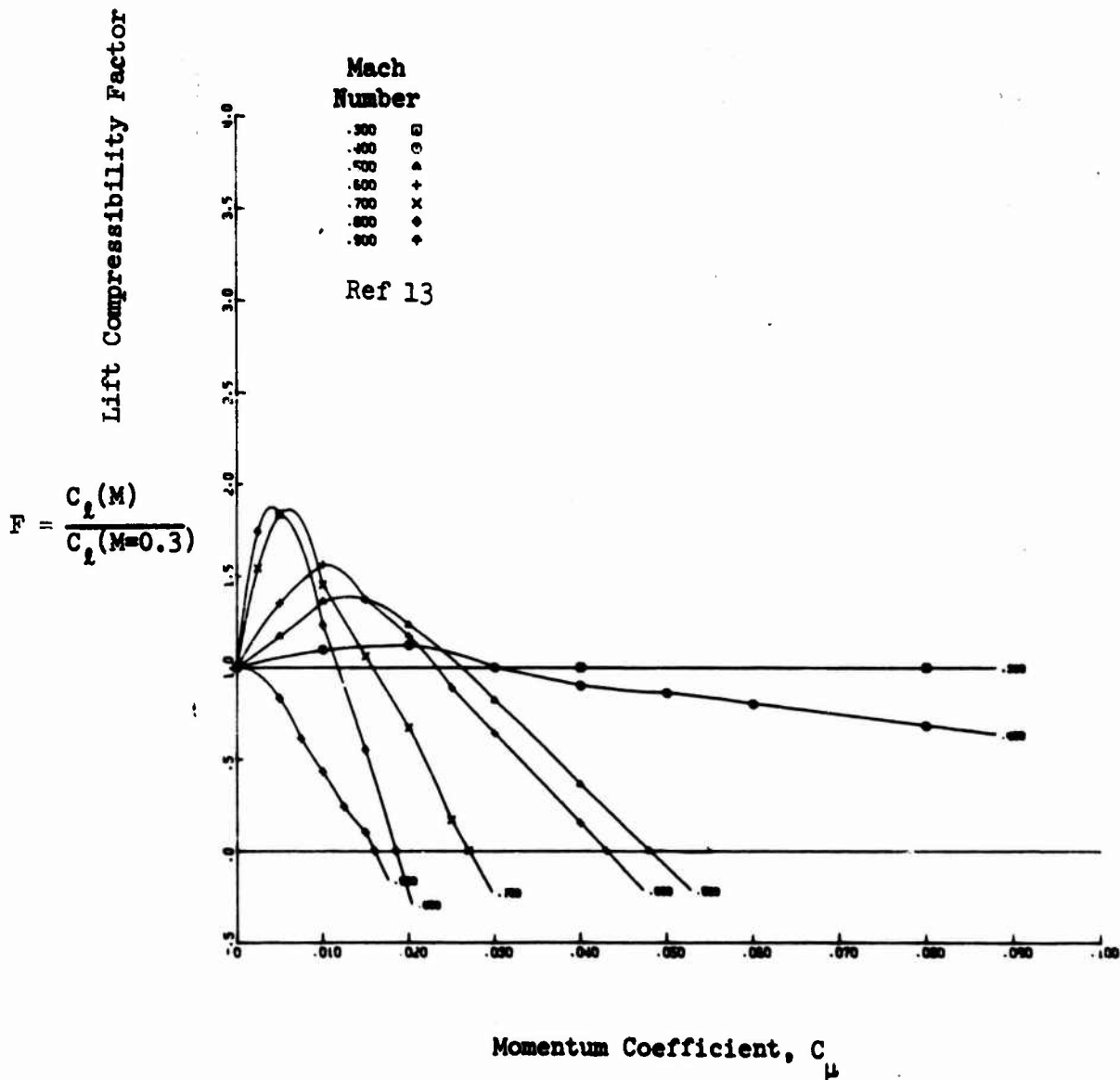


Figure A5 - Lift Compressibility Factor

(a)  $w/R_{TE} = 0.01209$

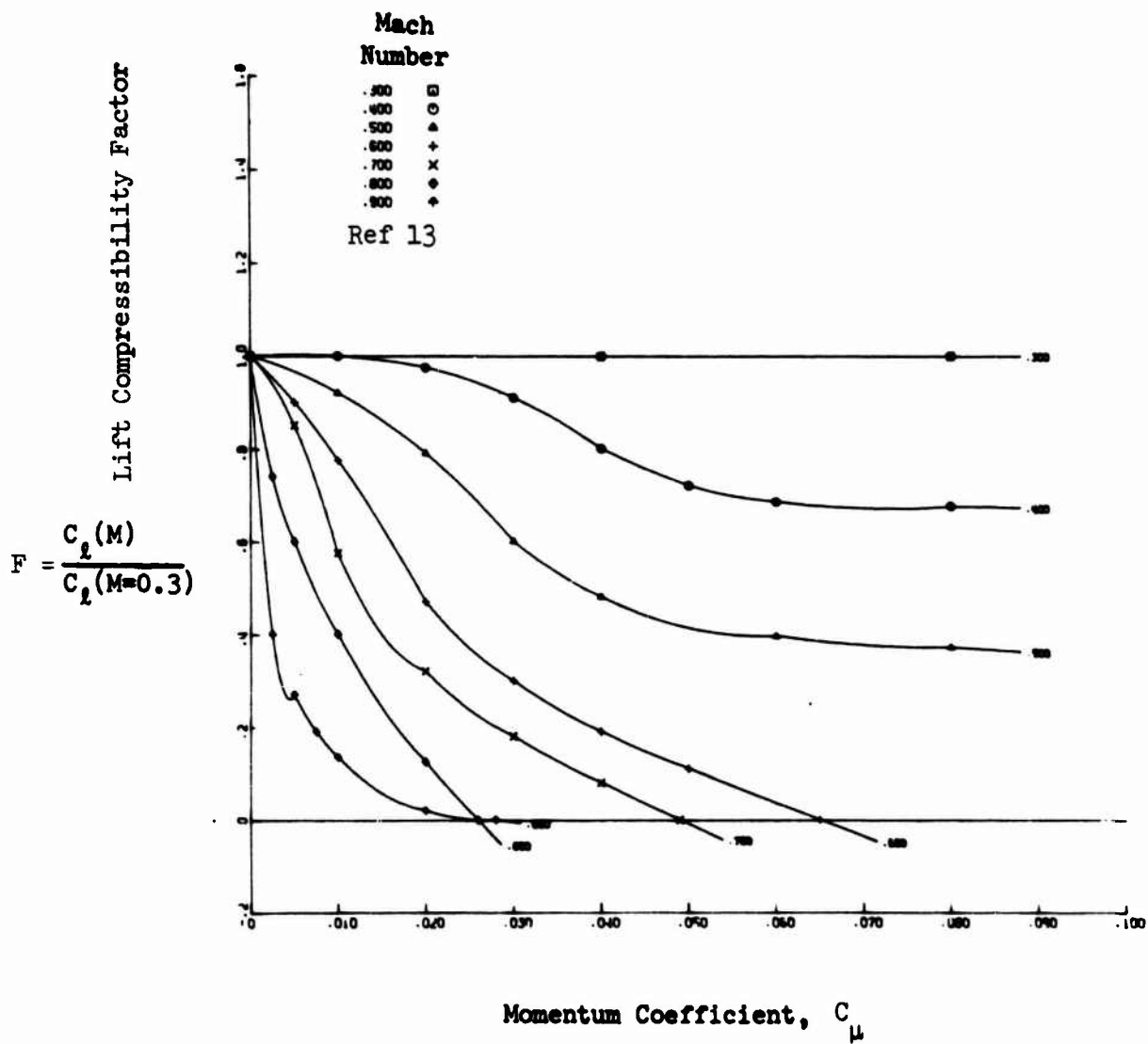


Figure A5 - (Concluded)

(b)  $w/R_{TE} = 0.0323$

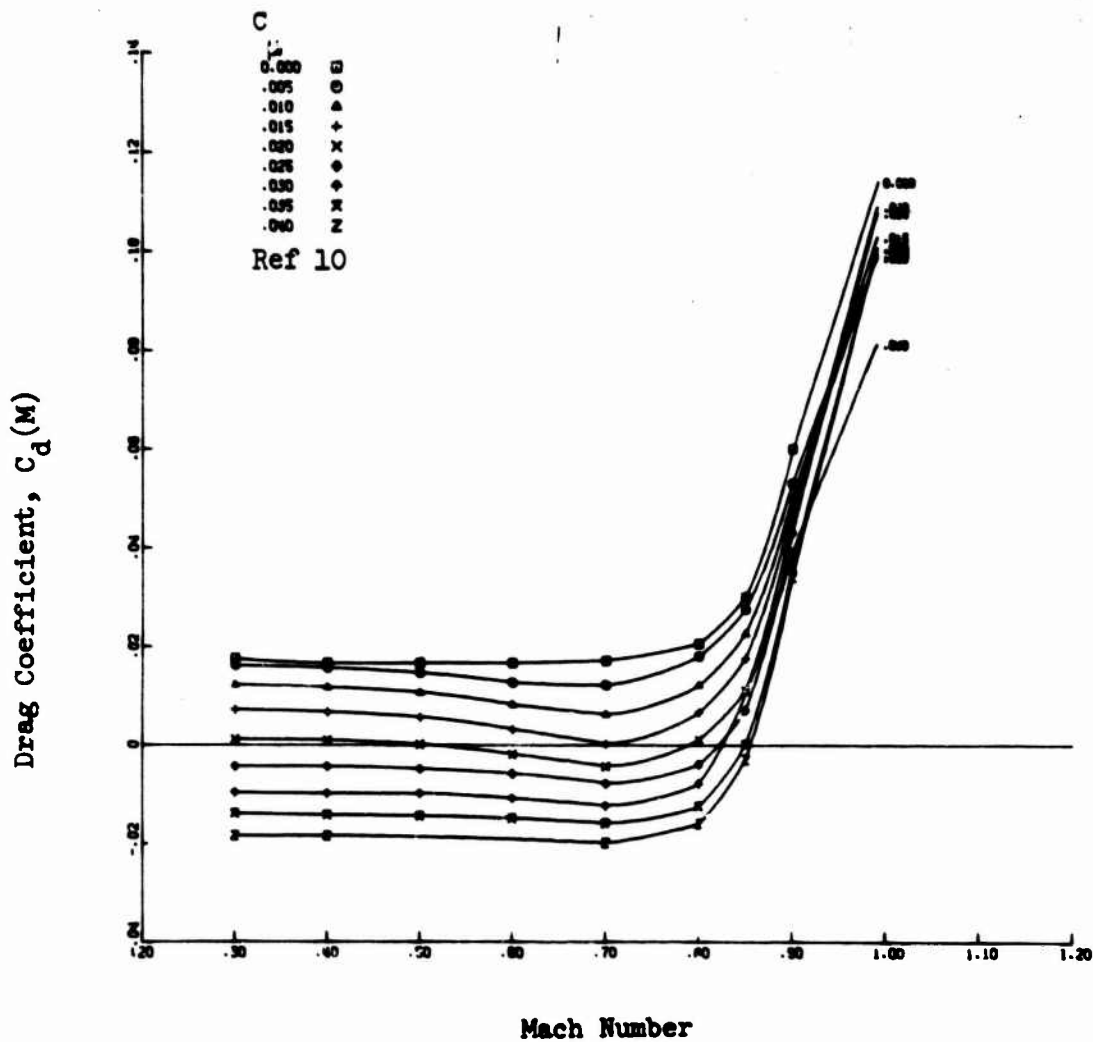


Figure A6 - Drag Compressibility Effect

(a)  $w/R_{TE} = 0.01209$

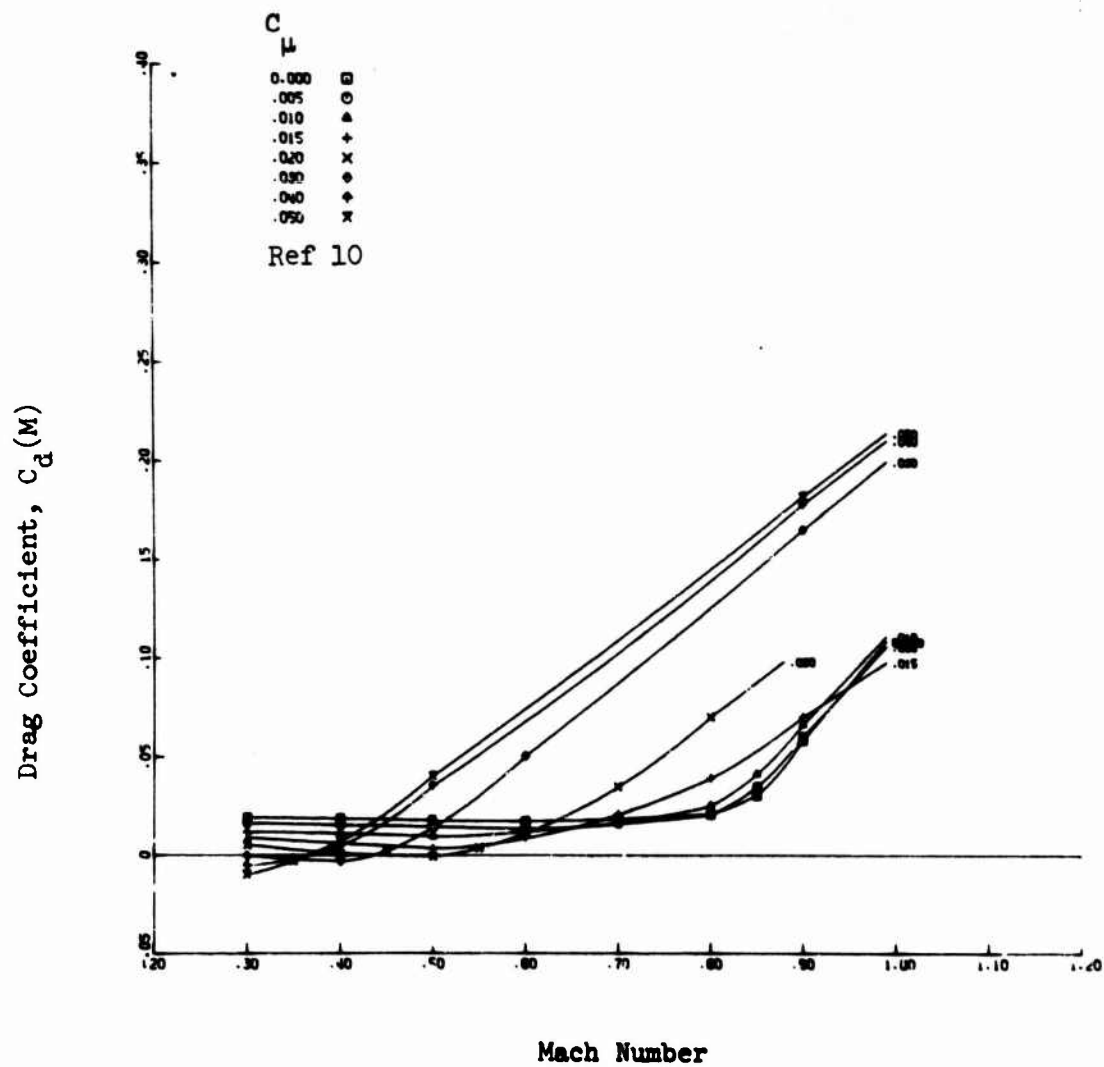


Figure A6 - (Concluded)

(b)  $w/R_{TE} = 0.0323$

# INITIAL DISTRIBUTION

## Copies

6	ONR	Chief of Naval Research Department of the Navy, Mail Stop #48 Attn: Aeronautics, Code 461 Washington, D. C. 20360
12	NAVAIR	Commander Naval Air Systems Command Department of the Navy, Mail Stop #287 Washington, D. C. 20360 1 NAVAIR 320 4 NAVAIR 604 1 NAVAIR 5104 1 NAVAIR 5302 1 NAVAIR 53011 1 NAVAIR 53012 1 NAVAIR 53014 1 NAVAIR 53031 1 NAVAIR 53032
1	NAVSEC	Commander Naval Ship Engineering Center Attn: CVAN Ship Design Manager (6103C1) Center Building Prince Georges Center Hyattsville, Maryland 20782
1	NRL	Director Naval Research Laboratory Attn: Technical Information Office Department of the Navy, Mail Stop #10 Washington, D. C. 20390
1	NRL	Director Naval Research Laboratory Attn: Library, Code 2029 (ONRL) Washington, D. C. 20390
1		Superintendent U. S. Naval Postgraduate School Monterey, California 93940
1		Commanding General U. S. Army Material Command Attn: AMCRD-FA Department of the Army Washington, D. C. 20315

Copies

2	DDC	Administrator Defense Documentation Center for Scientific and Technical Information Building #5, Cameron Station Alexandria, Virginia 22314
1		Commanding Officer U.S. Army Air Mobility Research and Development Laboratory Attn: SAVFE-AM Fort Eustis, Virginia 23604
1	NASA-Ames	U. S. Army Air Mobility Research and Development Laboratory NASA-Ames Research Center Attn: Technical Director Moffett Field, California 94035
2		U. S. Air Force Flight Dynamics Laboratory Wright-Patterson AFB, Ohio 45433 1 XFV, VTOL Technology Division 1 FXM, Aeromechanics Branch
2	NASA-Langley	National Aeronautics and Space Administration Langley Research Center Langley Station Hampton, Virginia 23365 1 Mr. John P. Campbell 1 Technical Library
2	NASA	National Aeronautics and Space Administration 600 Independence Avenue, S.W., Mail Stop #85 Washington, D. C. 20546 1 Code RAA 1 Mr. Alfred Gessow
3	NASA-Ames	National Aeronautics and Space Administration Ames Research Center Moffett Field, California 94035 1 Full Scale Research Division 1 Technical Library 1 Large Scale Aerodynamics Branch, Mark Kelly
1		Air Force Office of Scientific Research 1400 Wilson Boulevard Attn: Mechanics Division Arlington, Virginia 22209

Copies

1		U. S. Army Research Office Attn: Engineering Sciences Division Durham, North Carolina 27706
1		Director U. S. Army Advanced Materiel Concepts Agency 2461 Eisenhower Avenue Attn: AMXAM-SM or AMXAM-FT Alexandria, Virginia 22314
1	NATC	Commander Naval Air Test Center Dir., TPS Patuxent River, Maryland 20670
1	NADC	Commander Naval Air Development Center Attn: Technical Library Warminster, Pennsylvania 18974
1		Headquarters, U.S. Air Force (AFRDT-EX) Deputy Chief of Staff Research & Technology
1		Aviation System Command Department of the Army Attn: B. H. Boiron 12th and Spruce Streets St. Louis, Missouri 63103
1		DDR & E/OSD - Tactical Aircraft System Attn: Col. R. L. McDaniel Room 3E 1047 Pentagon, Mail Stop #103 Washington, D. C. 20301
1		Superintendent U. S. Naval Academy Annapolis, Maryland 21402
1		Dr. A. L. Slafkosky Scientific Advisor Commandant of the Marine Corps (Code AX) Washington, D. C. 20380
2	CNO	Chief of Naval Operations Navy Department Attn: Code 077 Washington, D. C. 20350

CENTER DISTRIBUTION

Copies

24	NAVSHIPRANDCEN	Commander Naval Ship Research and Development Center Bethesda, Maryland 20034
		1 Code 5640
		8 Code 5643
		5 Code 169, R. M. Williams
		10 Code 169

## DOCUMENT CONTROL DATA - R &amp; D

(Security classification of title, body of abstract and indexing annotation must be entered when the overall report is classified)

1. ORIGINATING ACTIVITY (Corporate author) Aviation and Surface Effects Department Naval Ship Research and Development Center Bethesda, Maryland 20034		2a. REPORT SECURITY CLASSIFICATION <b>UNCLASSIFIED</b>	
3. REPORT TITLE <b>ANALYSIS OF THE HOVER PERFORMANCE OF A HIGH SPEED CIRCULATION CONTROL ROTOR</b>		2b. GROUP	
4. DESCRIPTIVE NOTES (Type of report and inclusive dates) <b>9 Technical Note</b>			
5. AUTHOR (Last name, middle initial, first name) <b>10 Robert M./Williams</b>			
6. REPORT DATE <b>11 August 1971</b>		7a. TOTAL NO. OF PAGES <b>12 54p.</b>	7b. NO. OF REFS <b>29</b>
8a. CONTRACT OR GRANT NO. <b>17 RR011-05-04,</b> <b>WF 32-421-202</b> <b>690-011</b>		9a. ORIGINATOR'S REPORT NUMBER(S) <b>Technical Note AL-221</b> <b>14 TN-AL-221</b>	
9b. OTHER REPORT NUMBERS (any other numbers that may be assigned this report)			
10. DISTRIBUTION STATEMENT Distribution limited to U. S. Government agencies only; Test and Evaluation; August 1971. Other requests for this document must be referred to <b>NAV SHIP R+D Ctr Bethesda, Md 20034</b>			
11. SUPPLEMENTARY NOTES <b>16 ONR-PO-1-0140,</b> <b>NR-212-204</b>		12. SPONSORING MILITARY ACTIVITY Office of Naval Research Aeronautics, Code 461 Arlington, Virginia 22217	
13. ABSTRACT A method for calculating the detailed hover performance of any arbitrary circulation control rotor is presented. The method includes such higher order effects as non-uniform inflow, internal ducting losses and experimental airfoil data. Calculations were performed on an untwisted constant chord blade with varying section thickness and camber. Hover Figures of Merit exceeding 0.80 are calculated for this rotor at thrust coefficient to solidity ratios of 0.20. The optimum pitch angle is determined for each thrust coefficient. The effects of slot height and tip Mach number are also analyzed. A comparison is made with a conventional rotor system of the same solidity. <b>A</b>			

387 695 ✓

mt

14

KEY WORDS

LINK A

LINK B

LINK C

ROLE

WT

ROLE

WT

ROLE

WT

✓ Helicopter Rotor  
 ✓ Circulation Control Rotor  
 Boundary Layer Control  
 Hover Performance  
 High Lift Systems